The Dissertation Committee for Meghana Malur Certifies
that this is the approved version of the following dissertation:

HOST INNATE IMMUNE RESPONSE TO INFLUENZA A VIRUS INFECTION: ROLE OF LGP2 AND IMPORTANCE OF NS1:CPSF30 INTERACTION FOR VIRULENCE

Committee:

Robert M. Krug, Supervisor

Jon M. Huibregtse

Vishwanath R. Iyer

Christopher S. Sullivan

Rick Russell

HOST INNATE IMMUNE RESPONSE TO INFLUENZA A VIRUS INFECTION: ROLE OF LGP2 AND IMPORTANCE OF NS1:CPSF30 INTERACTION FOR VIRULENCE

by

Meghana Malur, B.E, M.S

Dissertation

Presented to the Faculty of the Graduate School of

The University of Texas at Austin

in Partial Fulfillment

of the Requirements

for the Degree of

Doctor of Philosophy

The University of Texas at Austin

December 2011

Dedication

To my husband Mahesh

To my parents Shrimathi and Venkatesh Shamanna Malur,

To my sister Deepika and brother-in-law Mukund

for their love and support

Acknowledgements

I would like to thank Dr. Robert M. Krug for his valuable guidance, constant encouragement and constructive inputs during the course of my graduate studies. I would also like to express my gratitude to all the committee members Drs. Jon Huibregtse, Vishwanath Iyer, Chris Sullivan and Rick Russell for their genuine interest in my research and their helpful suggestions. I would like to acknowledge Dr Ruben Donis at Centers for Disease Control and Prevention (CDC) and his team for their contributions towards the collaborative work done in the H5N1 virulence study.

I am grateful to the past and present members of the Krug lab, Drs. Rei-lin Kuo, Haripriya Sridharan, Tien-ying Hsiang, Ligang Zhou, Guifang Chen, Mark Collins, Jesper Marklund and Chen Zhao and graduate students, Bart Smith and Chien Hung Liu for their ideas and support during the course of my studies.

I have been fortunate to have had the support and encouragement of so many wonderful friends-Nancy, Shruthi, Sujoy, Raina, Proleta, Ashwini, Depika and Pritam. Last but not the least I would like to thank my wonderful parents, my sister Deepika and brother-in-law Mukund and my mother-in-law and father-in-law for their unconditional love and support throughout my studies. And most of all I would like to thank my husband Mahesh for his love, support and patience during my graduate work.

Host Innate Immune Response to Influenza A Virus Infection: Role of LGP2 and Importance of NS1:CPSF30 Interaction For Virulence

Meghana Malur, Ph.D

The University of Texas at Austin, 2011

Supervisor: Robert M. Krug

Influenza A viruses can cause a highly contagious respiratory illness in humans. Immediately after virus infection the innate immune response is initiated by binding of viral RNA species to RIG-I that leads to activation of IRF3 and NF-κB transcription factors and activation of interferon (IFN) transcription. LGP2 is a member of the RIG-I like receptor (RLR) family and is induced after virus infection. The role of LGP2 in virus infection is controversial: it has been reported to either positively or negatively affect RIG-I mediated signaling. The goal of this study was to determine whether LGP2 has a role during infection with influenza A viruses that have circulated in humans. We focused on two viruses expressing NS1 proteins that differ in their ability to inhibit IRF3 activation and IFN transcription; a H1N1 virus (Tx91) that inhibits IRF3 activation and a H3N2 virus (Ud) that does not. This study revealed that LGP2 has strikingly different roles during infection of mouse embryonic fibroblasts and human cells with these viruses. Specifically, LGP2 has no detectable role in H1N1 virus-infected cells, whereas it downregulates IFN synthesis in H3N2 virus-infected cells. Our results indicate that LGP2 acts as a negative regulator of the IFN response in influenza A viruses that activate IRF3. The NS1 protein also binds the 30kDa-subunit of the cleavage and polyadenylation

specificity factor-CPSF30, a protein required for 3′-end processing of cellular pre-mRNAs, thereby inhibiting production of mature IFN-β mRNA. The NS1 proteins of pathogenic 1997 H5N1 viruses lack two highly conserved residues (F103 and M106) that are needed to stabilize the NS1-CPSF30 complex. Instead their NS1 proteins have L at 103 and I at 106, resulting in non-optimal CPSF30 binding in infected cells. We demonstrated that strengthening CPSF30 binding by changing L and I to the consensus residues (F and M respectively) leads to a dramatic (300-fold) increase in lethality of the virus in mice. This increased virulence is associated with faster systemic spread of the virus. Microarray analyses revealed increased cytokine levels in extrapulmonary tissues, particularly the brain. These results highlight the importance of NS1:CPSF30 binding in modulating virulence in H5N1 viruses.

Table of Contents

List of Tables

List of Figures

CHAPTER 1: LITERATURE REVIEW

1.1 INFLUENZA VIRUSES

Influenza is a contagious respiratory illness caused by influenza viruses that result in significant morbidity and mortality throughout the world. There are three types of influenza viruses-A, B and C. Influenza A viruses infect birds and a wide range of mammals including humans, horses, pigs, seals and whales (Webster, Bean et al. 1992). Influenza B viruses infect humans and seals (Osterhaus, 2000) and Influenza C viruses infect humans and pigs (Yuanji and Desselberger, 1984). Influenza A viruses can be further divided into different subtypes based on the antigenic variation of the surface glycoproteins, hemagglutinin (HA) and neuraminidase (NA). Currently there are 16 known subtypes of HA (H1-H16) and 9 known subtypes of NA (N1-N9). All subtypes can be found in wild aquatic birds, the natural reservoir of influenza viruses.

The common symptoms of influenza infection are cold, chills, fever, muscle pain, sore throat, headache, coughing and general discomfort (http://www.cdc.gov/flu/). Although influenza virus infection causes mild symptoms, certain influenza A viruses can cause pandemics. There were four major human pandemics: the first was the 1918 "Spanish flu" in which approximately 40 million people died worldwide. The second was the 1957 "Asian flu" and the third was the 1968 "Hong Kong flu". These pandemics resulted in a significantly high mortality rate. The 2009 H1N1 influenza virus also known

as “swine flu” was declared a pandemic by the World Health Organization (WHO). It spread globally at an alarming rate but was not as lethal as the other pandemics. Pandemic influenza viruses usually result from gene reassortments between different strains, a process called “antigenic shift”. The reassortants encode proteins which are distinct from the previously circulating strains and as a result, there is little or no immune protection against them in the human population.

Avian viruses like the highly pathogenic influenza A H5N1 viruses occur mainly in birds and are highly contagious and deadly among birds. In general, avian influenza viruses rarely cause disease in humans. Of the few avian influenza viruses that have crossed the species barrier to infect humans, highly pathogenic avian influenza (HPAI) H5N1 has caused the largest number of detected cases of severe disease and death in humans. There are continual concerns that the current highly virulent H5N1 avian strain may adapt and acquire the ability for efficient poultry-to-human and human-to-human transmission and in the future become a serious threat (http://www.cdc.gov/flu).

1.2 STRUCTURE OF INFLUENZA A VIRUS

Influenza A viruses belong to the Orthomyxoviridae family of RNA viruses. This family of viruses also includes influenza B, C and D (Thogotovirus) viruses. Influenza viruses are enveloped, negative sense, single stranded, segmented RNA viruses. Both influenza A and B viruses contain eight genomic RNA segments, whereas influenza C contains only seven genomic RNA segments (Lamb and Krug, 2001). The influenza A virus particle or virion is 80-120 nm in diameter and usually roughly spherical, although

filamentous forms can occur (International Committee on Taxonomy of Viruses: "The Universal Virus Database, version 4: Influenza A"). Despite these varied shapes, the viral particles of all influenza viruses are similar in composition.

The structure of the influenza A virus particle is shown in Figure 1.1 (Lamb and Krug, 2001). The outermost layer of the influenza virion or the viral envelope is a phospholipid bilayer derived from the host cell membrane at the time of budding. The most striking feature common to influenza virions of all shapes and strains is a layer of spikes projecting radially outwards all over the surface. These 'spikes' are the two surface glycoproteins of influenza viruses, hemagglutinin (HA) and neuraminidase (NA). The HA is interposed by clusters of NA with a ratio of HA: NA of about 4-5:1. The rod shaped HA is encoded by segment 4 and has two important functions. It mediates binding of the virus to target cells (Skehel and Wiley, 2000; Whittaker, 2001) and allows for release of viral ribonucleoproteins (RNPs) into the cytoplasm of the host cell (Whittaker, 2001). The mushroom shaped NA encoded by segment 6 is required for enzymatic cleavage of the sialic acid group from host glycoproteins thereby facilitating release of newly formed viral progeny from the host cell (Lamb and Krug, 2001). HA and NA are antigens to which antibodies can be raised. In fact, influenza A viruses are classified into subtypes based on the antibody response to HA and NA (for example, H5N1, H3N2 etc.). The M1 protein/matrix protein is underneath the viral envelope and provides rigidity to the membrane. It is derived from segment 7 and is the most abundant viral protein. It binds to HA, NA and M2 proteins as well as the RNPs forming a bridge between the

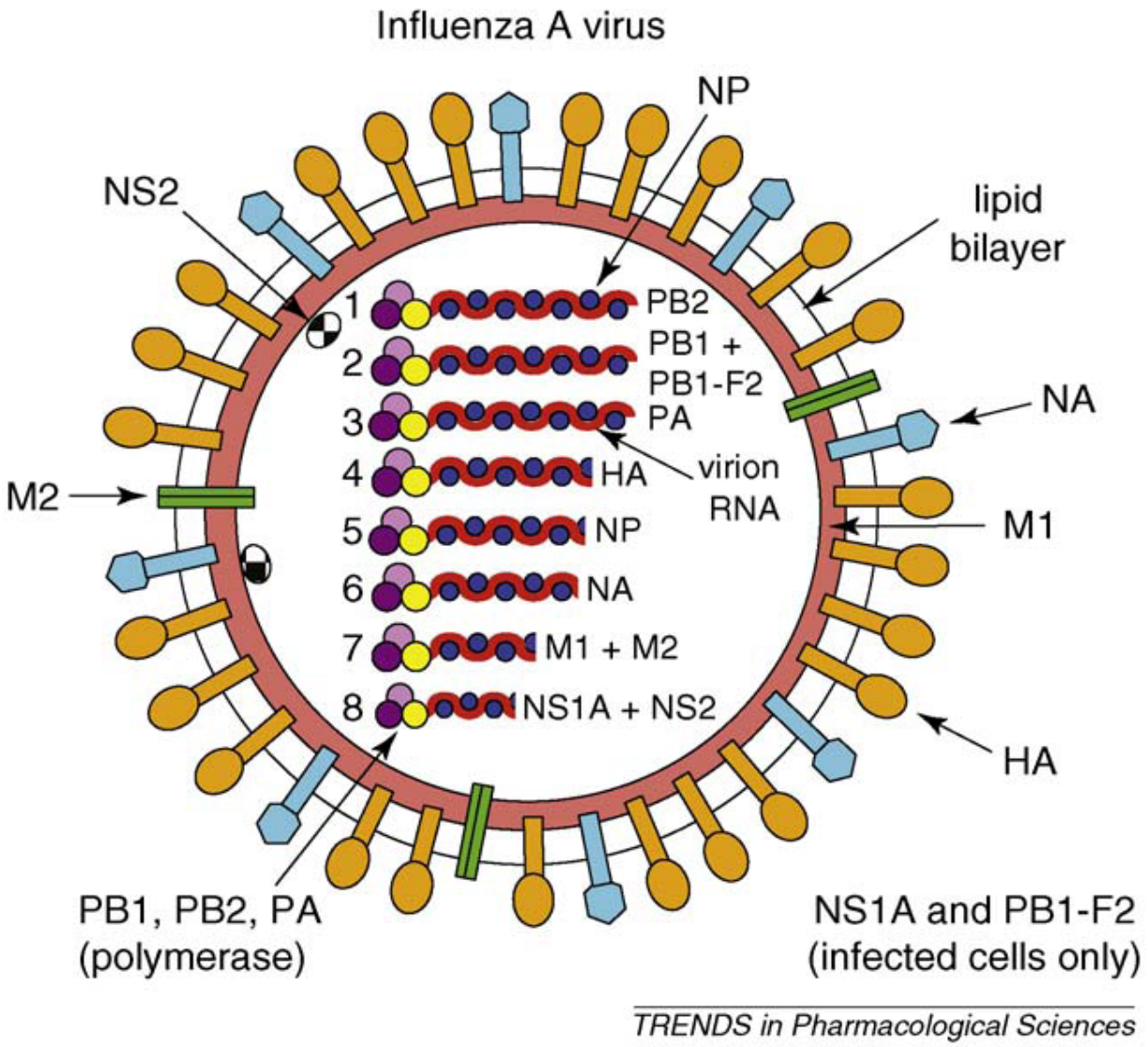

Figure 1.1 Schematic diagram of the structure of influenza A virion. The structural proteins, viral envelope, and the eight genomic RNA segments are indicated. The NS1A and PB1-F2 are found only in infected cells, and not in virions. Adapted from Noah and Krug 2005.

viral envelope and the core. M2 protein is encoded by a spliced mRNA derived from segment 7 and is an ion channel protein located in the viral envelope. M2 protein permits ions to enter the virion thereby mediating uncoating of the viral RNPs (Pinto and Lamb, 2006; Pinto and Holsinger, 1992). The nucleocapsid protein (NP) encoded by segment 5 is the major structural protein that interacts with the RNA segments to form the ribonucleoprotein (RNP). Each RNA segment is coated with NP, where one NP monomer interacts with approximately 20 nucleotides of the viral RNA (vRNA). The ends of the vRNA are looped back and bound to the viral polymerase complex comprising of PB1 (encoded by segment 2), PB2 (encoded by segment 1) and PA proteins (encoded by segment 3) (Figure 1.2). The viral core consists of vRNPs containing vRNA (minus strand), NP and the polymerase complex (PA, PB1 and PB2).

Similar to segment 7, segment 8 of influenza A virus encodes two proteins: non-structural protein 1 and 2 (NS1 and NS2/NEP (nuclear export protein)). The NS1 protein is expressed in large amounts in influenza A virus-infected cells but is not present in the virion hence the designation non structural (Lazarowitz, Compans et al. 1971) . NS1 is a multifunctional protein that participates in both protein-RNA and protein-protein interactions (Krug, Yuan W et al. 2003). It plays a crucial role in inhibition of the host antiviral response. The NS2 protein is generated by alternative splicing. It has a nuclear export signal (NES) and plays a role in the export of RNPs out of the nucleus in virus-infected cells (O'Neill, Talon et al. 1998).

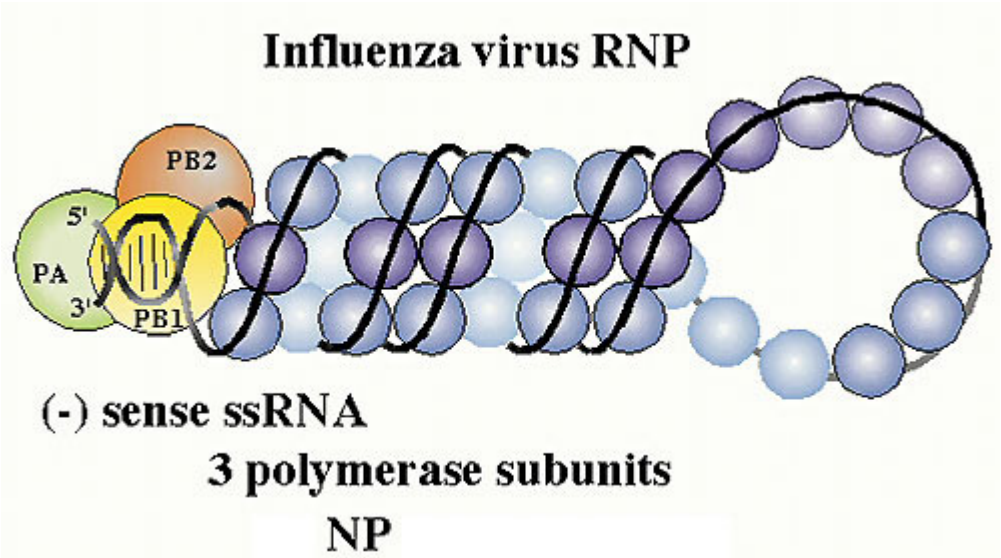

Figure 1.2 Structure of influenza viral RNP in the virion.
Blue spheres represent NP monomers binding vRNA (black line). The vRNA is looped back and forms a hairpin structure with a duplex (of 5′ and 3′ ends of vRNA) which forms the binding site for the polymerase subunits.http://www/microbiologybytes.com/virology/Orthomyxoviruses.html

The eight influenza A genomic segments encode 11-12 proteins. Segment 7 and 8 undergo alternative splicing to yield two proteins each. Segment 7 produces M1 and M2 and segment 8 produces NS1 and NS2 as described above. Viral mRNAs from segment 1 through segment 6 are monocistronic. However, the viral mRNA encoded by segment 2 of some viruses are known to encode two polypeptides in overlapping open reading frames: PB1, the polymerase, and PB1-F2, a short polypeptide expressed from an alternative +1 reading frame that seems to increase the virulence of some strains due to its involvement in induction of host-cell apoptosis (McAuley, Zhang et al. 2010). A third major polypeptide synthesized from PB1 mRNA via differential AUG codon usage was identified; PB1 N40 is a N-terminally truncated and functionally distinct variant of PB1 whose loss is detrimental to virus replication (Wise, Foeglein et al. 2009).

1.3 THE INFLUENZA VIRUS LIFE CYCLE

The influenza virus life cycle is shown in Figure 1.3 (Lamb and Krug, 2001). The virus binds to the host cell through interactions between it's HA and sialic acid sugars on the surfaces of host cells. The cell then imports the virus by endocytosis. In the acidic endosome, HA protein fuses the viral envelope with the vesicle's membrane, releasing the viral RNPs into the cytoplasm. Once released into the cytoplasm, these vRNPs are transported into the nucleus, which is the site of genome replication and transcription. The newly formed vRNPs are then exported from the nucleus by NS2 and M1. Viral assembly is facilitated by the membrane proteins HA, NA and M2 along with M1. The mature virus buds off from the cell with a coat of host phospholipid membrane

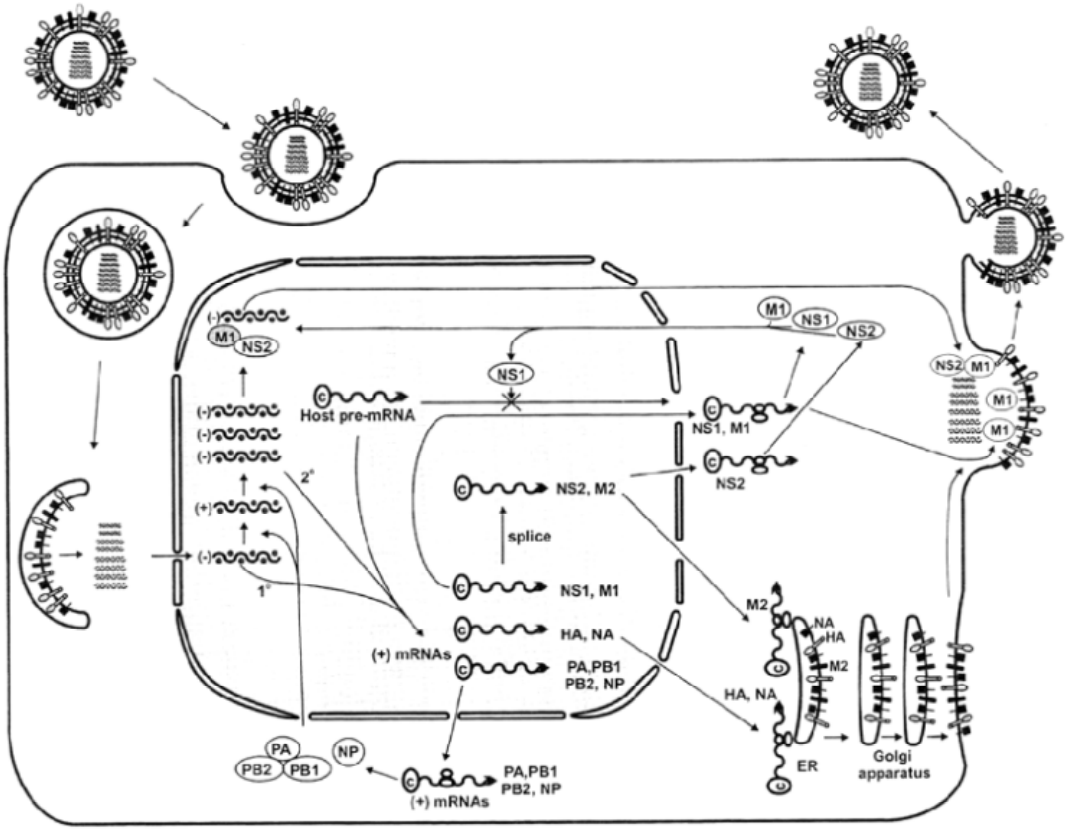

Figure 1.3 Life cycle of influenza virus.

The virus is endocytosed by the host cell, and in a pH dependent step, the vRNP is uncoated from the viral envelope. Transcription and Replication take place inside the nucleus. Virus assembly and budding take place in regions of the plasma membrane known as lipid rafts. Adapted from Lamb and Krug 2001.

consisting of HA and NA. As before, the viruses adhere to the cell through HA; the mature viruses detach once their NA has cleaved the sialic acid residues from the host cell. The details of each step in the viral life cycle are described below (Lamb and Krug, 2001)

Virus Adsorption, Entry and Uncoating

Influenza viruses bind to host cell receptor proteins that contain polysaccharides terminating with sialic acid. A sialic acid that is attached to galactose provides a recognition site for the virus's HA protein. This sialic acid can be connected at different positions on galactose. In nature, two major linkages are found between terminal sialic acid residues and the carbohydrates they are bound to in glycoproteins-α (2,3) and α (2,6). The avian influenza strain H5N1 recognizes mainly α (2,3)-linked version of the carbohydrate which is found in birds. In humans, such carbohydrates are found only in the lower respiratory tract, which may explain why the H5N1 strain though deadly, is rarely transmitted between humans. In contrast, the upper respiratory tract of humans contains mainly α (2,6)-linked receptors, and it is to these receptors that human influenza A viruses bind. Both α (2,3) and α(2,6)-linkages are found in swine (Ito, 2000). Therefore swine serves as a natural mixing vessel for avian and human influenza viruses, having the potential to produce novel, dangerous pathogenic viruses.

After the virion attaches to sialic-acid containing receptors at the cell surface, the virus-receptor complex is taken into cells by endocytosis. As the endosomal vesicles containing virus particles move towards the nucleus, their pH drops. This change in pH is

accomplished by H+ ATPases that pump protons into the vesicle. In the influenza virion, the vRNAs are bound to a number of viral proteins, including M1 protein. This protein forms a shell underneath the lipid membrane of the virion. If the vRNAs are bound to M1 protein they cannot enter the nucleus when they are released from the virion due to size constraints. In order to get around this problem, the influenza virion has a few copies of M2 protein in its membrane. M2 is a type III transmembrane protein that forms tetramers and whose transmembrane domains form a proton-selective channel (Lamb and Krug, 2001; Pinto and Lamb, 2006; Pinto, Holsinger et al. 1992)**.** The low pH environment activates the M2 ion channel. This channel allows proton conduction into the virion core, causing the dissociation of the RNP core from the underlying M1 protein, which allows for its subsequent import into the nucleus. Studies with the antiviral drug amantadine highlight the importance of the M2 protein. Amantadine binds to the transmembrane region of the M2 channel, thereby sterically blocking it and inhibiting the function of the M2 channel. This in turn, blocks the virus life cycle (Jing, Ohigashi et al. 2008; Wang, Takeuchi et al. 1993).

A critical step in virus life cycle is 'uncoating' of the virus. HA mediates virus-host membrane fusion and therefore plays an important role in viral uncoating. HA exists either in an uncleaved precursor form (HA0) or in a cleaved form consisting of two disulfide-linked chains (HA1 and HA2) (Lamb and Krug, 2001). HA1 contains the receptor binding domain and HA2 contains the fusion peptide. When the endosomal pH reaches 5.0, HA2 undergoes a folding event that exposes the 'fusion peptide' that is relocated more than 100 Angstroms towards the target membrane (Carr and Kim, 1994;

Hernandez, Hoffman et al. 1996). The fusion peptide can intercalate into the lipid bilayer, bringing both the viral and endosomal membranes into contact with each other. A number of trimeric HA molecules in the same region of the membrane mediate fusion between the viral and host membrane. The fusion process expels vRNPs into the host cytoplasm which are then imported into the nucleus (Whittaker, 2001).

Influenza viral transcription and replication occurs in the nucleus; therefore after being released into the cytoplasm, the vRNPs must enter the nucleus. The viral proteins that make up the vRNP are NP, PA, PB1 and PB2. All of these proteins have known nuclear localization signals (NLSs) that can bind to the cellular nuclear import machinery and thus enter the nucleus. (Akkina, Chambers et al. 1987; Jones, Reay et al. 1986; O'Neill, Jaskunas et al. 1995; Nieto, de la Luna et al. 1994)

Viral transcription and replication

The influenza viral genome is made up of negative sense strands of RNA. In order for the genome to be transcribed, it must first be converted into a positive sense RNA to serve as a template for the production of viral RNAs. The three largest vRNAs encode the three subunits of the RNA-dependent RNA polymerase- PA, PB1 and PB2. The polymerase is responsible for the transcription and replication of the eight segments of the viral RNA genome in the nuclei of infected cells. The presence of a functional polymerase complex in the infective virion particle is essential to initiate the first round of transcription and RNA replication because the negative-sense vRNA cannot be

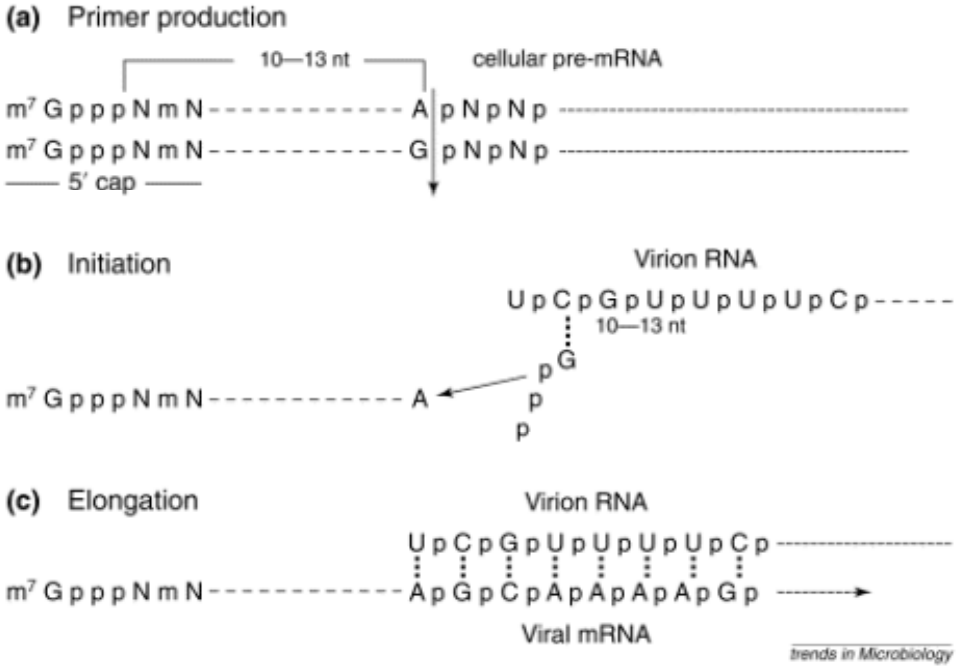

Figure 1.4 'Cap snatching' mechanism of influenza A polymerase.
A. Influenza A polymerase contains an intrinsic endonuclease activity which cleaves cellular mRNAs approximately 10-13 nucleotides downstream of 5′ end of the RNA. This releases the cap that is then used as primer for transcription of viral messages. B. During initiation, a G is added at the 3′ end of the cap structure after which elongation C. proceeds with the vRNA as template. Adapted from Chen and Krug, 2000.

directly translated into protein. The influenza polymerase is involved in two important reactions in the viral life cycle: transcription and replication.

Transcription

During transcription the PA-PB1-PB2 complex is localized in the nucleus of the infected cell. The process is primer-dependent, and the virus obtains the 5′-primer from the host by a unique mechanism called 'cap snatching'. PB1 subunit of the polymerase complex contains a functional binding site for the 5′-terminal sequence of vRNA. As a result of binding the 5′-terminal sequence of vRNA two new functions of the polymerase are activated (i) cap-binding activity of PB2: the PB2 subunit of the polymerase complex binds to the 5′, 7-methylguanosine cap of a host pre-mRNA molecule (ii) endonuclease activity of PA: the host pre-mRNA is subsequently cleaved 10-15 nucleotides downstream by the PA endonuclease. The resulting short capped RNA primer is used to initiate polymerization by the RNA-dependent RNA polymerase of the PB1 subunit using the 5′ and 3′-bound vRNA as template (Dias, Bouvier et al. 2009; Li, Rao et al. 2001; Yuan, Bartlam et al. 2009). The viral polymerase complex elongates viral mRNA until reaching a stretch of 5 to 7 uridine (U) residues located 15-22 nucleotides before the 5′ end of the vRNA template. After reiteratively copying the U-track at the 5′ end of vRNA template, the viral polymerase generates the 3′-polyadenylated tail for the viral mRNAs in a host-independent process (Plotch, Bouloy et al.1981; Poon, Pritlove et al. 1999). In this manner capped polyadenylated positive-sense mRNAs that resemble host cell messages are generated. These chimeric viral mRNAs are exported from the nucleus to the cytoplasm for translation.

Viral replication

The vRNA templates are transcribed into complementary RNA (cRNA), which is neither capped nor polyadenylated, but instead is a complete copy of the template. These cRNAs then form the template for synthesis of further vRNA segments that are packaged into progeny virions. Viral RNA replication occurs in two steps: first a full-length copy of the vRNA is produced, termed cRNA (positive sense). This is then copied back into negative sense vRNA segments. The synthesis of cRNAs and vRNAs is initiated without a primer, in contrast to the initiation of viral mRNA synthesis (Honda, Ueda et al. 1988; Medcalf, Poole et al. 1999; Shapiro and Krug, 1988). The function of NP during RNA synthesis which has received the most attention is its role in the switch from mRNA transcription to genome replication. To switch from the synthesis of viral mRNAs to that of cRNAs, it is necessary to change from capped RNA-primed initiation to unprimed initiation and to prevent termination and polyadenylation at the poly (A) site. Three models have been proposed to explain this switch (Portela and Digard, 2002; Vreede, Jung 2004)**.** The encapsidation hypothesis proposes that NP does not have any control over the switch; instead NP is merely an essential co-factor that is required to co-transcriptionally coat the nascent cRNA segments. The template modification hypothesis proposes that the interaction of a soluble NP with the template RNA alters its structure and thereby brings about the switch. However, biochemical studies showed that NP binds directly to the polymerase and alters the transcriptional function of the polymerase through direct protein-protein contacts (Newcomb, Kuo et al. 2009). Therefore NP function is best explained by the 'polymerase modification model'.

Export of viral RNPs

Once the vRNPs are synthesized, they are exported from the nucleus into the cytoplasm for assembly and budding. For nuclear export of proteins, the formation of a ternary complex composed of the export substrate, a cellular export factor, CRM1 and Ran-GTP is crucial. The viral proteins essential for export are M1 and the NS2/NEP (O'Neill, Talon et al. 1998). NS2 binds to M1 and export is mediated as vRNP-M1-NS2 complex through the nuclear pore (Boulo, Ruigrok et al. 2007; Neumann, Hughes et al. 2000; Wang, Takeuchi et al. 1993).

Assembly and Budding

First the viral mRNAs are translated to produce all the proteins needed to generate a new virion particle. The mRNAs encoding the envelope proteins, HA and NA glycoproteins and M2 are translated by ribosomes on the endoplasmic reticulum (ER). Once the proteins are made, they are transported to the cell membrane via small vesicles that eventually fuse with the plasma membrane. Influenza viruses, utilize lipid raft domains in the plasma membrane of infected cells as sites of virus assembly and budding (Scheiffele, Rietveld et al. 1999). Lipid rafts are cholesterol and sphingolipid-enriched regions of the plasma membrane. Only HA and NA appear capable of altering the membrane curvature, thereby initiating the budding event. The cytoplasmic tails of HA and NA then serve as docking sites for M1 which in turn coats the vRNPs.

The cytoplasmic tail of M2 plays an important role in binding to M1 although the recruitment of M2 to sites of virus budding may involve associations with both M1 and HA. In addition to vRNP recruitment, interactions between M1 and M2, or M2 and HA

are important in membrane scission. Membrane scission and the release of the budding virion require the M2 protein. The delay in M2 expression is thought to allow for the initiation of budding and for proper virion assembly, before scission and virion release occurs. Following the completion of membrane scission, NA cleaves sialic acid off the cell surface, preventing the HA—receptor interaction and freeing the budded virion (Lamb and Krug, 2001).

1.4 TREATMENT OF INFLUENZA VIRUSES

Immunization with an inactivated vaccine or a live attenuated vaccine is the most effective way to provide protection against influenza. Seasonal influenza vaccines are composed of three influenza viruses that are predicted to be most common during the upcoming season. Vaccinations are provided annually since influenza viruses are constantly changing and the influenza vaccine has to be updated from one season to the next to protect against the most recent and most commonly circulating viruses. So, for optimal protection against influenza, annual vaccination is recommended (www.cdc.gov/flu).

There are four licensed prescription influenza antiviral agents available in the United States: amantadine, rimantidine, zanamivir and oseltamivir (www.cdc.gov). Zanamivir and oseltamivir are related antiviral medications in a class of medications known as neuraminidase inhibitors. These two medications are used in the treatment and prophylaxis of influenza caused by both influenza A and B viruses. The trade name for zanamivir is Relenza and the mode of usage is oral inhalation. Zanamivir binds to the

active site of the NA protein and prevents viral release and spread. The design of highly effective inhibitors of NA became feasible when analysis of the three-dimensional structure of influenza NA revealed the location and structure of the catalytic site. Zanamivir is a potent NA inhibitor which closely mimics the natural substrate fitting into the active site pocket and engaging the protein in the most energetically favorable interaction. Oseltamivir is a prodrug, a relatively inactive chemical which is converted into its active form by metabolic process after it is taken into the body. It is sold under the trade name Tamiflu and is the first orally active NA inhibitor, serving as a competitive inhibitor to sialic acid. Although no influenza seasonal or pandemic strains have shown any signs of resistance to zanamivir, seasonal H1N1 influenza A viruses, excluding the 2009 H1N1 virus, have acquired resistance to oseltamivir.

Amantadine (trade name Symmetrel) and a closely related derivative of adamantine, Rimantadine (trade name Flumadine) have similar biological properties. Amantadine interferes with the function of the viral M2 ion channel protein which is required for 'uncoating' of the virion particle once it has been endocytosed by the host cell. At later stages of the viral infection, these drugs act on the HA molecule to induce a premature pH-induced conformational change in HA. According to the CDC, most influenza A strains have shown resistance to adamantanes and amantadine is no longer recommended for treatment of influenza. The potential threat of a pandemic coupled with increasing number of influenza strains acquiring resistance to existing antivirals has stimulated increased research on developing new antivirals against influenza A viruses.

Recently, functional and structural studies have led to the discovery of novel targets for the development of antivirals, specifically the NS1 protein, NP and the viral polymerase.

1.5 NON-STRUCTURAL PROTEIN 1 (NS1) OF INFLUENZA A VIRUSES

The non-structural protein 1 (NS1) of influenza A viruses is a multifunctional protein that is widely regarded as an antagonist to host immune responses (Egorov, Brandt et al. 1998; Honda, Ueda et al. 1988; Kochs, García-Sastre et al. 2007). It also plays a role in virulence during infection (Chapter 3) and has other effects on virus replication and temporal regulation of viral RNA synthesis. The NS1 protein is not present in the virion but is expressed at very high levels in the infected cell (Krug and Etkind, 1973). It is encoded by segment 8, which upon splicing results in a second polypeptide namely, NS2. Both NS1 and NS2 share 10 N-terminal amino acids (Lamb and Lai, 1980). The ratio of NS1:NS2 is 10:1 and this regulation in splicing is thought to be controlled partially by NS1 itself (Garaigorta, 2007). In infected cells, NS1 predominantly localizes to the nucleus, but a significant proportion can also be found in the cytoplasm (Greenspan, Palese et al. 1988; Newby, Sabin et al. 2007), particularly at later times post infection (Garaigorta, 2007; Melén, Fagerlund et al. 2007). Some NS1 proteins contain one nuclear localization signal , whereas other NS1 proteins contain two nuclear localization sequences (NLS1 and NLS2) which mediate active nuclear import via binding to cellular importin-α (Melén, Fagerlund et al. 2007). NS1 has a strain-specific length of 230-237 amino acids and an approximate molecular mass of 26 kDa. The NS1 protein is composed of two distinct functional domains: the N-terminal RNA

binding domain (RBD), (amino acids 1-73) and a C-terminal 'effector' domain (amino acids 74-237). Each of these domains is described in detail below.

RNA binding domain of NS1

The N-terminal RBD of NS1 possesses all the dsRNA binding activities of the full length protein. Both NMR and X-ray crystallography of this domain have revealed that it is a symmetric homodimer which forms a six-helix chain fold. Due to this unique structure, the NS1 protein is different than other dsRNA binding proteins. The dimeric NS1 protein binds the dsRNA duplex with a 1:1 stoichiometry yielding a complex with a dissociation constant (K_d) of ~1 μM which is relatively low compared to other dsRNA binding proteins (Chien, Xu et al. 2004). Arginine at position 38 (R38) in the NS1 protein has been shown to be critical for RNA binding activity. Consequently, mutating arginine at this position to alanine completely abolishes dsRNA binding *in vitro* (Wang, Riedel et al.1999).

Furthermore, studies with a recombinant virus with a mutation at position 38 from R to A showed that the primary role of dsRNA binding by the NS1A protein in virus-infected cells is to protect the virus against the antiviral state induced by interferon alpha or beta (IFN-α/β). Specifically, the dsRNA-binding activity of the NS1 protein is responsible for rendering influenza A virus resistant to the antiviral activity of the 2′-5′ OAS/RNase L pathway. OAS is activated by dsRNA, a putative by-product of viral replication and polymerizes ATP into 2′-5′-oligoadenylate chains. These chains cause dimerization and activation of the latent RNase, RNase L, which inhibits virus replication by degradation of RNA (Silverman, 2007). Because the activation of RNase L is

completely dependent on the dsRNA activation of 2′-5′ OAS, it is likely that the primary role of dsRNA binding by the NS1 protein is to sequester dsRNA away from 2′-5′ OAS (Min and Krug, 2006).

Effector domain of NS1A

The C-terminal effector domain of NS1 binds to several host factors: PKR, the 30kDa subunit of cleavage and polyadenylation specificity factor (CPSF), poly (A) binding protein II (PABII) and PI3-kinase (PI3K). NS1 can directly block the function of the dsRNA-dependent serine/threonine protein kinase R (PKR). Specifically, substitution of residues 123 and 124 in NS1 was shown to prevent the NS1-mediated binding and inhibition of the dsRNA-activated antiviral protein kinase, PKR. Thus this mutant virus induced PKR activation and exhibited reduced viral protein synthesis at late times post-infection. Surprisingly, this mutation also enhanced viral RNA synthesis, indicating that NS1 also plays a role in controlling viral RNA replication during infection (Min, Li et al. 2007).

NS1 directly binds to two zinc-finger domains in the 30kDa subunit of CPSF30 (Nemeroff, Barabino et al. 1998; Noah, Twu et al. 2003; Twu, Noah et al. 2006). As a result, NS1 sequesters CPSF30 from binding cellular pre-mRNAs, thereby inhibiting cleavage and polyadenylation of the 3′-end of host cell pre-mRNAs, including IFN-β pre-mRNA. As polyadenylation of influenza A virus mRNAs is independent of cellular 3′ end processing factors, viral mRNAs are not affected by inhibition of CPSF30 function. Structural studies have highlighted the importance of G at position 184 in the interaction between CPSF30 and NS1. A mutation at position 184 from G to R completely abolishes

CPSF30 binding to NS1 protein. Two amino acids that lie outside the binding pocket, namely F103 and M106 have also been shown to be important for stabilizing this interaction between CPSF30 and NS1 (Das, Ma et al. 2008).

An important role of the NS1 protein is to counter host cell antiviral responses. A major cellular antiviral response is the synthesis of interferon-α/β which in turn activates an array of genes encoding proteins that establish an antiviral state (Goodbourn, Didcock et al. 2000; Haller, Kochs et al. 2006). Using a novel assay to measure IFN-β transcription, it was shown that the ability of the NS1 protein to block the activation of IRF3 and IFN-β transcription differs markedly between HN subtypes. This striking difference in the ability of NS1 proteins to block the activation of IRF3 and IFN-β transcription is mediated largely by the C-terminal region of the effector domain (amino acids 183-230/237). This C-terminal region contains only one amino acid that covaries with the functional difference: amino acid 196 is E in the NS1 proteins that block activation of IRF-3 and IFN-β transcription, whereas it is K in the NS1 proteins that do not block these activations (Kuo, Zhao et al. 2010). Clearly the NS1 protein uses more than one countermeasure to inhibit the IFN response within the host.

NS1 binds to and activates phosphotidylinositol 3 kinase (PI3K) which results in the activation of PI3K effector Akt. This leads to subsequent inhibition of caspase 9 and glycogen synthase-kinase 3β, and inhibition of the virus-induced apoptotic pathway (Ehrhardt and Ludwig, 2009)**.** The temporal regulation of pro and anti-apoptotic function of NS1 is important: inhibition of apoptosis at early times after infection might be

beneficial for the virus whereas promoting apoptosis at later times postinfection might allow for more efficient spread of progeny virions.

1.6 HOST IMMUNE RESPONSES

The immune response in vertebrates is divided into two categories: innate and adaptive immune response. The adaptive immune response in vertebrates involves antibody production, induction of cell-mediated immunity and immunological memory. The main mediators of this response are clonally expanded T and B lymphocytes that are generated by gene rearrangements and hyper mutations. The innate immune response is the first line of defense against invading pathogens in the host and is described in more detail below.

1.6.1 Innate immunity

Pathogen-associated molecular patterns (PAMPs) are recognized with the help of different pattern recognition receptors (PRRs). In the case of virus infection this recognition leads to increased inflammatory response, cytokine production and establishment of an antiviral state in the host. The innate immune response consists of three families of pathogen sensors: Toll-like receptors (TLRs), NOD-like receptors (NLRs) and RIG-I like receptors (RLRs) (Thompson, Kaminski et al. 2011). Members of the TLR family recognize bacteria, viruses, fungi and protozoa. To date, there are 10 members in the TLR family in humans and 13 members in mice. Individual TLRs interact with different combinations of adaptor proteins and activate various

transcriptional factors such as Nuclear factor (NF)-κB, activating protein-1 (AP-1) and interferon regulatory factors (IRFs), driving a specific immune response. NLRs detect only bacteria and certain NLRs like NOD1 and NOD2 activate NF-κB, a key transcriptional factor for inflammatory and immune gene expression. RLRs detect only viruses, specifically viral nucleic acids and activate IRF family members and NF-κB.

1.6.2 RIG-I like receptor (RLR) family

Once viruses enter the cytoplasm, viral RNA species are sensed by members of the RIG-I-like receptor (RLR) family. The three members of this family are-retinoic acid inducible gene-I (RIG-I), melanoma differentiation associated gene 5 (MDA5) and laboratory of genetics and physiology 2 (LGP2). The RLRs belong to the superfamily 2 (SF2) helicases/ATPases (Gorbalenya and Koonin 1988). RIG-I and MDA5 share a number of similarities with respect to their domains. They have (i) a N-terminal region consisting of two caspase activation and recruitment domains (CARDs), (ii) a central DExD/H box RNA helicase domain which can hydrolyze ATP (iii) a repressor domain (RD) embedded within the C-terminal domain (CTD) that in the case of RIG-I is involved in auto- regulation. MDA5 does not encode a RD that self-regulates its signaling actions. Instead interactions between MDA5 and specific regulatory proteins might serve to mediate its signaling control (Diao, Li et al. 2007). The third member in this family, LGP2, contains a DExD/H helicase domain and a CTD, but lacks the CARD domains (Figure 1.5).

The roles of RLRs in the detection of RNA viruses have been established through analyses of mice deficient for each respective RLR. RIG-I is essential for the recognition of different viruses such as, Influenza A virus, Vesicular Stomatitis irus (VSV), Sendai virus, (SeV), Hepatitis virus and Japanese encephalitis virus (JEV). MDA5 is required for the recognition of other RNA viruses, including picornaviruses such as Encephalomyocarditis virus (EMCV), Mengo virus and Theiler's virus. Mice deficient for RIG-I and MDA5 are consistently more susceptible to infection with the respective viruses than wild-type mice are. This suggests that RIG-I and MDA5 have specificities in their detection of RNA viruses, presumably through recognition of distinct structures of viral RNA (Kato, Takeuchi et al. 2006). So far, the exact RNA ligand that is recognized by MDA5 remains largely uncharacterized although a study showed that under physiological conditions a complex RNA-structure activated MDA5 (Pichlmair, Schulz et al. 2009).

1.6.3 RIG-I: a sensor for influenza A viruses

RIG-I was initially identified to be a pattern recognition receptor (PRR) for viral RNA by screening of cDNA libraries for factors that induce Interferon β (IFN-β) promoter

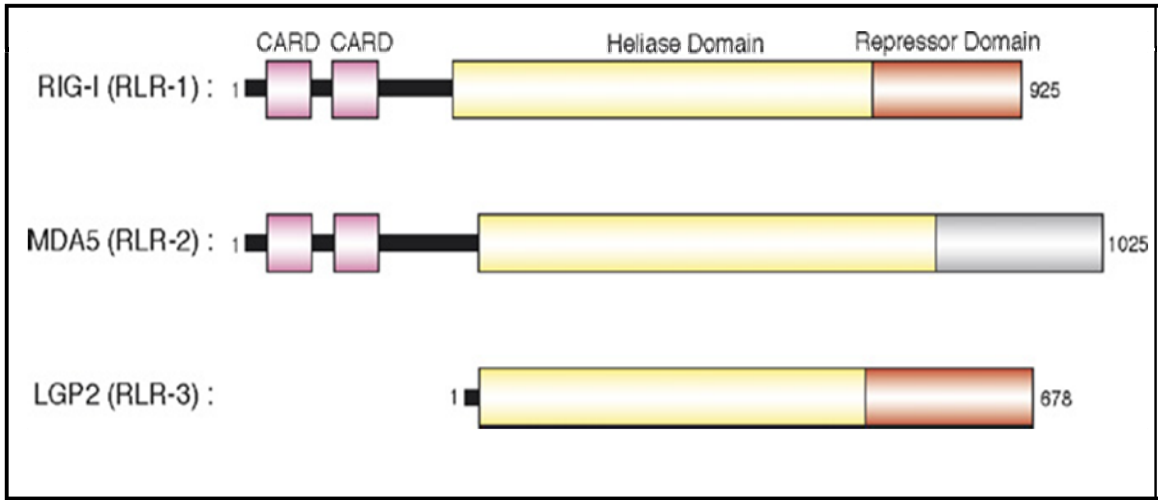

Figure 1.5 Different domains of the RIG-I like receptor family (RLRs).
RIG-I and MDA5 have N-terminal CARD domains, a central helicase domain and a CTD. LGP2, the third member of this family lacks the CARD domains. Adapted from Yoneyama and Fujita, 2007.

expression in response to the viral dsRNA mimic poly I:C (Yoneyama, Kikuchi et al. 2004). There are at least two important motifs that must be present on RNA in order for RIG-I to distinguish between "self" and "non-self" (i) RIG-I preferentially recognizes RNA sequences marked with 5′ tri-phosphorylated (5′ppp) ends which sets it apart from "self" RNA because free 5′ ppp RNA ends are absent from eukaryotic cytoplasm due to mRNA capping. The 5′ tri-phosphate is important since removal of this motif or modifications with mono and di-phosphate groups severely attenuate signaling (Hornung, Ellegast et al. 2006; Pichlmair, Schulz et al. 2006; Rehwinkel, Tan et al. 2010; Schlee, Roth et al. 2009; Schmidt, Schwerd et al. 2009)**.** In the case of influenza, at least one phosphate group is required for triggering RIG-I signaling but the 5′ tri-phosphate is required for full activation of the RIG-I pathway. (ii) A short complementary sequence or polynucleotide motif is also required since only a synthetic 5′ ppp ssRNA failed to drive RIG-I signal activation (Schlee, Roth et al. 2009).

1.6.4 RIG-I structure and activation

Recently there were several studies that revealed the structure and function of the various domains of RIG-I (Civril, Bennett et al. 2011; Kowalinski, Lunaski et al. 2011; Luo, Ding et al. 2011; O'Neill and Bowie, 2011). Duck RIG-I (dRIG-I) (Kowalinski, Lunaski et al. 2011), human RIG-I lacking the CARD domains with dsRNA (Luo, Ding et al. 2011), mouse RIG-I with an ATP analogue (Civril, Bennett et al. 2011) and human RIG-I with dsRNA and an ATP analogue (Jiang, Ramanathan et al. 2011) were studied. The overall structures from these studies are similar. The helicase domain of RIG-I

contains two helicase RecA-like domains-Hel1 and Hel2. There were two interesting features identified (i) A novel insertion domain Hel2i present in Hel2 that is required for dsRNA interactions (ii) and a long "elbow"-like structure, called "pincer", which is V-shaped and composed of 2 long α helices. It grips an α-helical shaft that extends from Hel1 and connects Hel1 to the CTD. The structures revealed the mechanical communication that occurs between the various proteins domains, Hel1, Hel2 and the CTD of RIG-I and how the movement of these domains results in activation of RIG-I.

The RIG-I structure in complex with dsRNA showed that the protein domains surround the dsRNA and that RIG-I binds the duplex RNA like beads on a string. Hel2 and Hel2i form a single rigid body unit and Hel2i is an important component of the ring that grips dsRNA by directly interacting with the minor groove of the RNA backbone. Hel1, Hel2 and CTD also clasp duplex RNA and Hel1 binds to both strands of RNA at the same time. Hel2 and the CTD are connected by the pincer. The pincer is not involved in direct RNA binding nor is it a part of the ATPase core. Instead it acts as a bridge transmitting information between domains and hence is essential for RNA sensing. This was clear when mutations in pincer reduced the RNA-stimulated IFN response (Kowalinski, Lunaski et al. 2011).

The repressor domain (RD) of RIG-I initially identified as amino acids 735-925 was further delimited to amino acids 747-801 which corresponds to part of the pincer

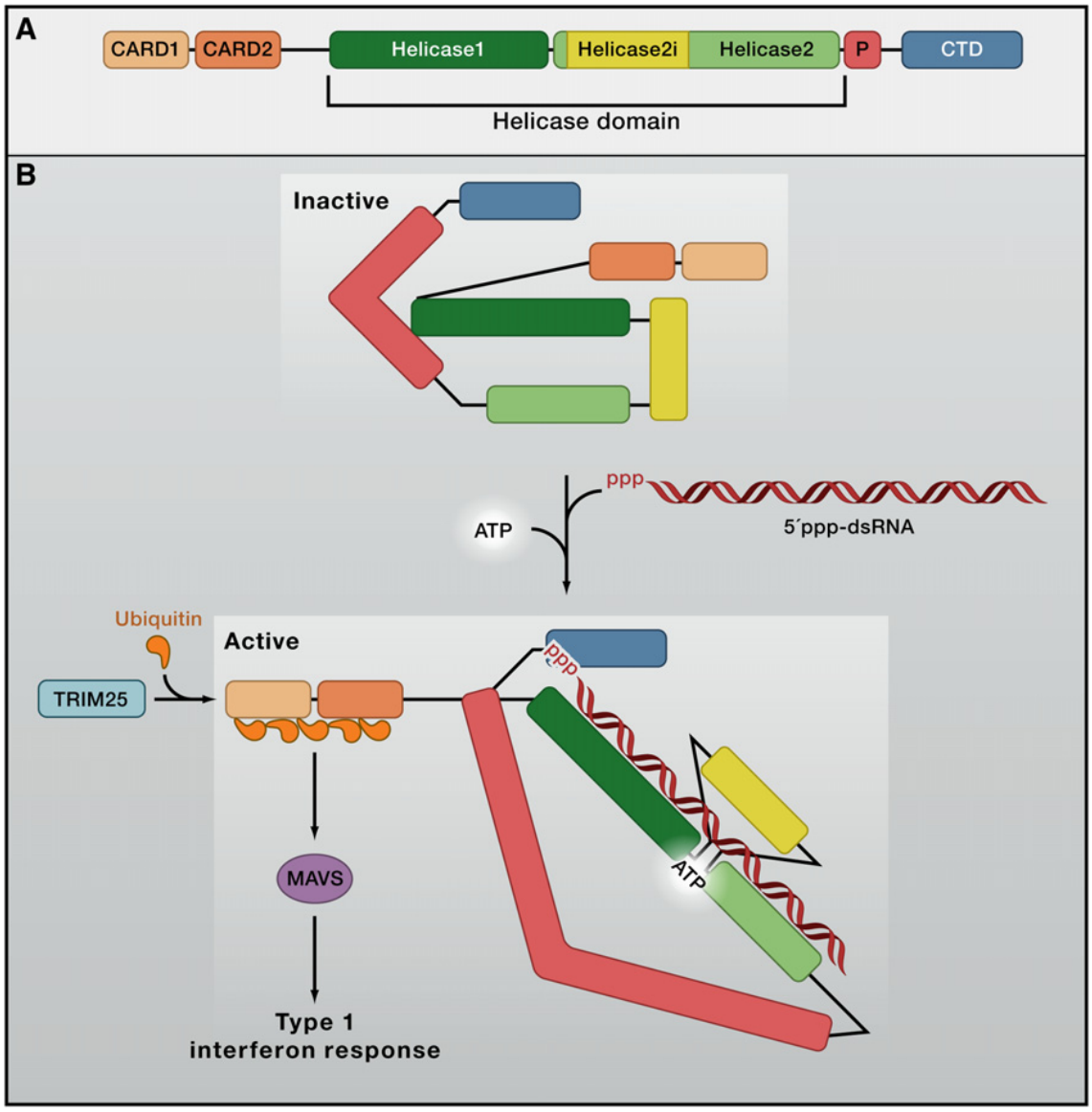

Figure 1.6 Model for RIG-I activation.
RIG-I undergoes a conformational change such that the previously hidden CARD domains are exposed and can interact with the downstream signaling partner IPS-1 via CARD-CARD interactions. Adapted from O'Neill and Bowie, 2011.

domain connecting the helicase and the CTD of RIG-I. Alanine substitutions of the conserved residues in the pincer domain conferred constitutive activity to full-length RIG-I. Interestingly, the constitutive active mutants did not exhibit ATPase activity, suggesting that ATPase is required for de-repression but not signaling (Kageyama, Takahashi et al. 2011). The conservation of all motifs and the helical pincer in LGP2 indicates that the structural models presented for RIG-I can provide a good framework to understand and analyze LGP2 function.

Based on the above structural and biochemical studies, a model for RIG-I activation has been proposed. In the inactive state, the RIG-I CARDs are sequestered by the helicase domains and are not available for signaling. The CARDs are bound to the Hel2i subdomain and the CTD is flexibly linked to the rest of the protein and is available to interact with RNA. Initial capture of 5′-triphosphate dsRNA by the CTD would then increase the concentration of dsRNA in the vicinity of the helicase. The inner face of the CTD cavity is positively charged and therefore can accommodate the dsRNA. Cooperative dsRNA and ATP binding results in a dramatic conformational change of the RIG-I helicase domain such that all three sub-domains move relative to each other. This rearrangement brings Hel1 and Hel2 into close contact with each other, resulting in a high-affinity complex between dsRNA and the helicase domain. The pincer is proposed to open and close or rotate thereby altering the orientations of Hel1 to Hel2 and CTD to Hel1. This pushes the tandem CARDs away from the helicase complex. Therefore changes in the structure of pincer are thought to contribute to the transmission of the signal to the CARDs. The CARDs are subjected to E3 ligase tripartite motif-containing

25 (TRIM25)-dependent K63 polyubiquitination of Lys172 (Gack, Shin et al. 2007) or endogenous K63-linked polyubiquitin chain binding (Zeng, Sun et al. 2010). The polyubiquitinated CARDs of RIG-I interact with IPS-1 by CARD-CARD interactions. This leads to downstream signaling and production of type I IFN induction. RNF125, another ubiquitin ligase, is a negative regulator of RIG-I and mediates K48-linked polyubiquitination of RIG-I, leading to the degradation of the RIG-I protein by proteasomes (Arimoto, Takahashi et al. 2007).

1.6.5 RIG-I signaling pathway

Almost immediately after sensing the virus via the cytoplasmic sensor, RIG-I, the host mounts an antiviral response, which occurs in two phases: the first is an immediate early IFN-independent phase and the second phase is mediated by IFN (Haller, Kochs et al. 2006).

1.6.6 IFN-independent early antiviral response

The first antiviral response occurs prior to the production of interferon and does not require viral protein synthesis (Boyle, Pietropaolo et al. 1999; Kim, Latham et al. 2002; Navarro, Mowen et al. 1998; Yoneyama, Suhara et al. 1998). The Interferon regulatory factor 3 (IRF3) and IRF7 transcription factors are activated and are translocated to the nucleus. They form a transcription complex called VAF (virus-associated factor) together with the transcriptional co-activators p300 and CREB-binding protein. This complex binds to the IFN-stimulated response elements (ISREs) in the

promoters of certain cellular antiviral genes, e.g., the genes for ISG15 and 2′-5′-oligo (A) synthetase (OAS), thereby inducing their transcription (Kim, Latham et al. 2002; Navarro, Mowen et al. 1998). The antiviral proteins produced through this early IFN-independent immune response provide initial protection to the infected cells against viral replication. In most cell types except for plasmacytoid dendritic cells, IRF3 is constitutively expressed whereas IRF7 expression remains low until it is induced in the presence of IFN in a positive feed-back loop. IRF3 is therefore thought to function in the immediate early enhanceosomes in most cell types whereas IRF7 directs later transcription programs (Hiscott, 2007).

Virus infection also activates transcription factors that in turn activate IFN-α/β genes. The interaction between activated RIG-I and IPS-1 leads to recruitment of TNFR-receptor associated factor 3 (TRAF3) and Fas-associated death domain-containing protein (FADD). This complex signals to TBK1 and IKKi to phosphorylate and activate IRF3 and IRF7. Signaling through the IPS-1/TRAF3/FADD complex also activates caspases 8 and 10 leading to IKK complex activation along with recruitment of NF-κB essential modulator (NEMO) and release of the inhibitory IκB from the NF-κB complex. NF-κB can then enter the nucleus to activate cytokine genes. NF-κB also drives transcription of the IFN-α/β genes together with IRF3 and AP-1 (Du, 1992; Fujita, Miyamoto et al. 1989; Suhara, Yoneyama et al. 2002; Du and Thanos, 1993).

1.6.7 Antiviral response mediated by interferons

IFN-β (IFN) that is produced and secreted as a result of RLR signaling cascade is an important cytokine produced by the host defense system. IFN was originally identified as a secreted protein that can "interfere" with viral replication within the host. IFNs bind to the receptors on cell surfaces and activate cellular signaling cascades which serve to limit further spread of the disease.

Classification of interferons

Based on the type of receptor through which they signal, human interferons have been classified into three major types: I, II and III. Type I IFNs in humans contain 14 IFNα subtypes, IFNβ, IFNδ, IFNε, IFNζ, IFNκ, IFNo and IFNτ. All type I IFNs bind to a ubiquitously expressed heterodimeric receptor, IFNAR (IFNα receptor), which consists of IFNAR1 and IFNAR2. The type II IFN only has a single IFN γ gene and is secreted by T cells and NK cells. The dimer of IFN γ proteins bind to a tetramer consisting of 2 IFNγ receptor 2 (IFNGR2) and 2 IFNγ receptor 1 (IFNGR1) chains. Type III IFNs have three interferon lambda (IFN λ) subtypes (IFNλ1, IFNλ2, IFNλ3 also referred to as interleukin (IL)-29, IL-28A and IL-28B respectively) that signal through IFN λ receptor 1 (IFNLR1; also known as IL-28Rα) and interleukin-10 receptor 2 (IL-10R2, also known as IL-10R).

Type I IFN Signaling

IFN α and β of type I IFNs play a crucial role in innate immunity and also have a preparatory function for the subsequent adaptive immune response. The importance of type I IFN was seen in mice with targeted deletions of the type I IFN receptor. These mice succumbed to infection faster despite having a normal adaptive immune system.

Therefore the type I IFN system is essential for vertebrates to control and combat viral infections (Haller, Kochs et al. 2006).

Once the IFN α/β protein is synthesized and secreted, it exerts its effect through an autocrine or a paracrine manner. It can bind to the IFN α/β receptors to direct Janus kinases/Signal transducers and activators of transcription (JAK-STAT) signaling and ISGF3-dependent expression of interferon-stimulated genes (ISGs). Prior to activation, tyrosine kinase 2 (Tyk2) and the tyrosine kinase JAK1 associate with IFNAR1 and IFNAR2, respectively. IFN binding to the receptor causes dimerization of the receptor and activates Tyk2 and JAK1 which phosphorylate STAT1 and STAT2. Phosphorylated STAT1 and STAT2 form a stable heterodimer and translocate into the nucleus where they associate with a monomer of IRF-9 to form the ISGF3 heterotrimer that binds to the IFN-stimulated response element (ISRE) present in the promoter of IFN responsive genes and induces transcription.

Type II IFN signaling is similar to type I IFN. In Type II IFN signaling, subunits of IFN γ receptor, IFNGR1 and IFNGR2, are associated with JAK1 and JAK2 respectively. IFN γ binding to the receptor activates JAK1 and JAK2 and results in the formation of STAT1-STAT1 homodimer that translocates into the nucleus and binds to the gamma-activation sequence (GAS) of ISGs to stimulate transcription. Binding of this homodimer to GAS does not require IRF9. However, IFN γ can activate several ISRE-containing promoters, including CXCL10 by activating the formation of the heterotrimer containing IRF9 and STAT1-STAT1 homodimer.

The interferon stimulated genes (ISGs) include those encoding proteins with direct antiviral activity such as viperin, ISG56 and IFIT family of proteins, OAS and Mx-1 as well as numerous pro-inflammatory cytokines and chemokines. The transcriptional up-regulation of several hundred ISGs as well as amplification of the IFN response by increases in the expression of IFN-α subtype occur by means of a positive feedback loop. All these events contribute in controlling infection and establishing an antiviral state.

1.7 LGP2/DHX58

Laboratory of genetics and physiology 2 (LGP2) was originally identified in a study that explored the evolutionary relationship between Drosophila-signal transducers and activators of transcription (d-Stat), Zebrafish-Stat (z-Stat) and three of the seven mammalian STATs (STAT 3,5a,5b). Zebrafish Stat3 (z-Stat3) gene and a 500-kb region spanning mouse chromosome 11, 60.5cM were isolated, sequenced and analyzed. Within this region four new genes were identified one of them being Lgp2 (Miyoshi, Cui et al. 2001). Subsequently, Lgp2 was characterized as a cytoplasmic protein of 678 amino acids that shares similarities with members of the DEAD/H box family of proteins (Cui, Li et al. 2001). LGP2 shows 31 and 41% amino acid identities to the helicase domains of RIG-I and MDA5, respectively (Yoneyama, Kikuchi et al. 2005). LGP2 is expressed in a wide spectrum of vertebrate genomes including fish, zebrafish, chickens and humans. LGP2 is induced upon a variety of stress signals like viral or bacterial infection and interferon treatment (Pollpeter, Komuro et al. 2011; Rothenfusser, Goutagny et al. 2005; Saito, Hirai et al. 2007; Yoneyama, Kikuchi et al. 2004).

When the RNA-binding activity of the C-terminal domains (CTDs) of the RLRs was compared by electrophoretic mobility shift assays (EMSAs) the LGP2 CTD bound to dsRNA and 5′ triphosphorylated–ssRNA with higher affinity than RIG-I and MDA5. LGP2 binds to other ligands such as dsRNA as seen in the structure of LGP2 CTD in complex with an 8-bp dsRNA (Li, Ranjith-Kumar et al. 2009). It has the highest affinity for dsRNA followed by RIG-I and MDA5. Specifically, LGP2 CTD binds dsRNA with 5′ overhangs, but not 3′ overhangs. However, another study showed that the end structure of dsRNA does not affect recognition by LGP2 (Takahasi, Kumeta et al. 2009). Further analyses are required to determine the mechanism of dsRNA recognition by LGP2 CTD.

The crystal structure of the regulatory domain of LGP2 has been determined (Pippig, Hellmuth et al. 2009) and is shown in Figure 1.6. The regulatory domain (RD) of LGP2 is a globular, slightly flattened domain with a concave and convex side. It consists of two four-stranded (β1, β2, β9, β10 and β5, β6, β7, β8) β sheets and one two-stranded (β3, β4) anti-parallel β-sheet. The three β-sheets are connected by small 3_{10} helical turns. The C-terminus contains a short α-helix (α1). The four stranded β-sheets are laterally connected by two protruding loops, each containing two highly conserved cysteine residues (Cys556 and Cys559 and Cys612 and Cys615). The four thiol groups of these cysteines (C556, C559, C612 and C615) coordinate the zinc ion in each of the four molecules in the asymmetric unit. In this study, LGP2 RD was shown to bind dsRNA in a 5′-triphosphate –independent manner. The binding affinity of LP2 RD to RNA duplexes is similar or even higher than the affinity of RIG-I RD for 5′-triphosphate RNA,

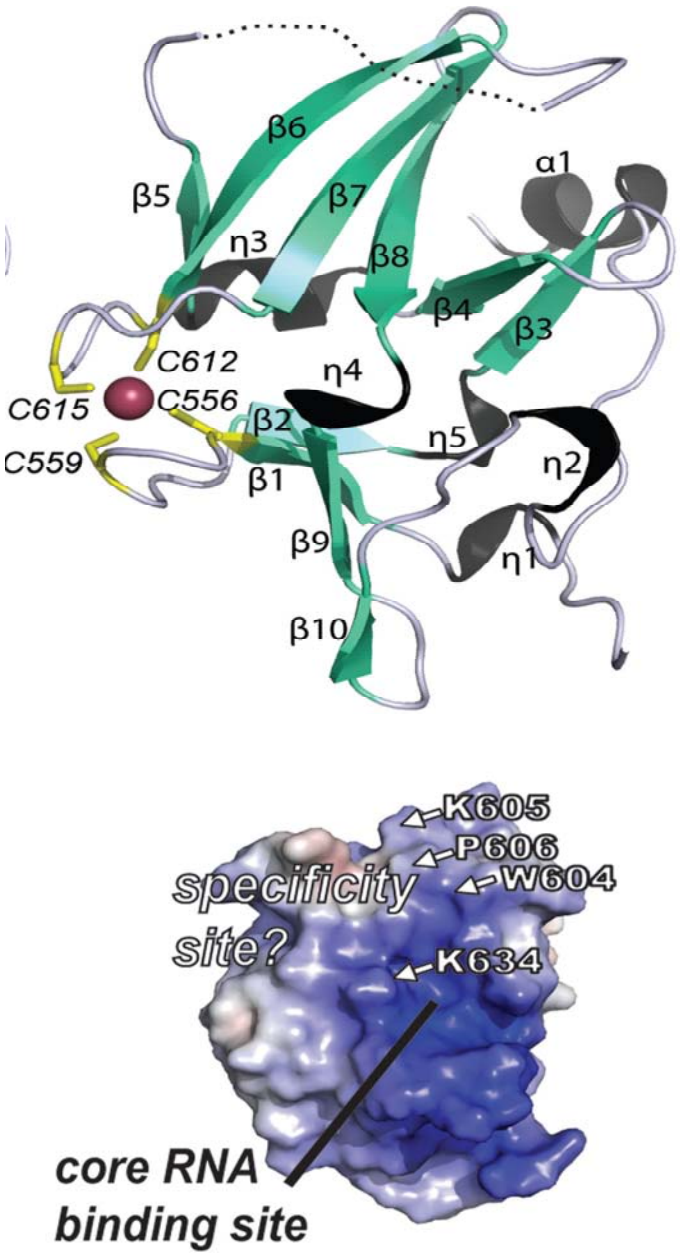

Figure 1.7 Structure of the repressor domain (RD) of human LGP2
A. Ribbon model of LGP2 RD B. Concave surface identified is the RNA binding site of LGP2 RD. Adapted from Pippig, Hellmuth et al. 2010.

indicating a physiologically relevant interaction. A "core RNA binding site" was predicted and the RDs of RIG-I and LGP2 were compared. However the construct used for RIG-I consisted of amino acids 801-925 which does not correspond to the newly delimited RD of RIG-I (Kageyama, Takahashi et al. 2011).

A previous study showed that full length LGP2 and LGP2 RD (amino acids 476-678) prevented Sendai virus induction of the IFN-β promoter and ISG56 expression in a manner similar to the RIG-I RD (amino acids 735-925). Therefore LGP2 RD is thought to have a negative regulatory effect on RIG-I signaling and the IFN response (Saito, Hirai et al. 2007). Two other mechanisms have been proposed describing the negative effect mediated by LGP2 which ultimately lead to inhibition of the IFN response: (i) LGP2 binds with higher affinity than either RIG-I or MDA5 to dsRNA and ssRNA via the CTD (Li, Ranjith-Kumar et al. 2009; Murali, Li et al. 2008; Pippig, Hellmuth et al. 2009). Since LGP2 lacks the CARD domains, it is not able to stimulate IFN transcription and competes with RIG-I for binding to RNAs (ii) LGP2 binds to a domain at the C terminus of IPS-1 and prevents recruitment of IRF3-phosphorylating kinase IKKi. This in turn inhibits activation of IRF3 and IFN transcription (Komuro and Horvath, 2006). Majority of the experiments in these studies were done *in vitro.* The negative role of LGP2 during vesicular stomatitis virus (VSV) infection was demonstrated *in vivo.* The induction of type I IFN was slightly augmented in LGP2-/- mice. Furthermore, mice lacking LGP2 exhibited resistance to VSV infection which is recognized by RIG-I (Venkataraman, Valdes et al. 2007).

However, recently LGP2 was reported to play a positive role in sensing RNA viruses recognized by RIG-I, such as vesicular stomatitis virus (VSV) and Sendai virus (SeV) as well as picornaviruses recognized by MDA5 such as EMCV and mengovirus. Overexpression of the CARDs from RIG-I and MDA5 in LGP2-/- mouse fibroblasts activated the IFN-β promoter, suggesting that LGP2 functions upstream of RIG-I and MDA5. Interestingly, LGP2 was reported to have no role in innate immunity during influenza A virus infection. There were no differences detectable in IFN-β production measured by ELISAs in wt and LGP2-/- mouse embryo fibroblasts (MEFs). Northern assays also showed similar levels of IFN-β and CXCL10 production in wt and LGP2-/- MEFs (Satoh, Kato et al. 2010). The influenza A/PR8/ΔNS1 virus was used in this study. Previous studies have shown that this mutant virus is extremely attenuated in IFN-competent systems. Thus this mutant virus only displays high pathogenicity in mice lacking antiviral mediators such as STAT1 or PKR (Garcia-Sastre, Egorov et al. 1998). The NS1 protein is an essential component of the virus defense machinery against the host. Lack of this gene would dramatically alter the virus-host interaction and the outcome of virus infection. Therefore it is important to determine whether LGP2 has a role in influenza A virus infection with a naturally occurring virus which has no deletions of any of the gene segments and that is the goal of my research (Chapter 2).

CHAPTER 2: LGP2 DOWNREGULATES THE PRODUCTION OF INTERFERON DURING INFECTION BY H3N2 INFLUENZA A VIRUSES

2.1 INTRODUCTION

Innate immunity against many viruses is initiated by the binding of viral RNA species to the repressor and helicase domains of RIG-I, a cytosolic protein that also contains two amino-terminal caspase activation recruitment domains (CARDs) (Yoneyama, Kikuchi et al. 2004; Yoneyama, Kikuchi et al. 2005). The RIG-I CARDs then associate with the CARDs of IPS-1, a mitochondrial-associated protein, thereby triggering the signaling pathway that leads to the activation of the IRF3 and NF-κB transcription factors and the activation of interferon (IFN) transcription (Fujita, Onoguchi et al. 2007; Meylan, Curran et al. 2005). LGP2 has repressor and helicase domains similar to those of RIG-I, but lacks CARDs, and hence cannot trigger the signaling pathway that leads to the activation of IFN transcription (Cui, Li et al. 2001; Yoneyama, Kikuchi et al. 2005).

The role of LGP2 in virus infection is controversial: it has been reported to either positively or negatively affect the RIG-I-mediated activation of IFN transcription and the production of IFN in virus-infected cells (Saito, Hirai et al. 2007; Venkataraman, Valdes et al. 2007). Influenza A virus, which utilizes the RIG-I-initiated pathway, was reported to be unique in that the production of IFN in infected cells was not affected by LGP2, unlike other viruses. These experiments used an attenuated H1N1 A/PR/8/34 (PR8) virus

that does not encode the NS1 protein (Satoh, Kato et al. 2010). A major role of the multifunctional NS1 protein is to counter the host antiviral response, including the synthesis of IFN. Consequently, infection with this attenuated PR8 virus results in robust activation of IRF3 and IFN synthesis **(**Garcia-Sastre, Egorov et al. 1998; Talon, Horvath et al. 2000). It was reported that the same amount of IFN was produced in wild-type and LGP2-/- mouse embryo fibroblasts (MEFs) infected with this attenuated PR8 virus, indicating that LGP2 has no role in infection with this attenuated virus.

Our goal was to determine whether LGP2 has a role during infection with wild-type, non-attenuated influenza A viruses that have circulated in the human population. Currently circulating H1N1 and H3N2 viruses differ in the ability of their NS1 proteins to inhibit the activation of IRF3 and IFN transcription (Kuo, Zhao et al. 2010). The NS1 proteins of H1N1 viruses that have circulated since 1979 block the activation of IRF3 and IFN transcription, whereas the NS1 proteins of all tested H3N2 viruses do not block these activations. For the present study we primarily focused on two viruses: a 1991 H1N1 virus (A/Texas/36/91, Tx91), and a 1972 H3N2 virus (A/Udorn/72, Ud). The NS1 proteins of these two viruses share the property of binding the 30-kDa subunit of the cellular cleavage and polyadenylation specificity factor (CPSF30), a protein that is required for 3′ end processing of cellular pre-mRNAs, and hence both NS1 proteins inhibit the 3′ end processing of IFN-β pre-mRNA.

Here we show that LGP2 has strikingly different roles during infection of MEFs and human cells with H1N1 and H3N2 influenza A viruses. Specifically, LGP2 has no

detectable role in H1N1 virus-infected cells, whereas it downregulates the synthesis of IFN in H3N2 virus-infected cells.

2.2 MATERIALS AND METHODS

Cell lines

A549 human lung carcinoma cells (ATCC CCL-185), Madine-Darby canine kidney (MDCK) (ATCC CCL-34) and HeLa cells (ATCC-CCL-2) were purchased from ATCC. These cell lines were cultured in DMEM (GIBCO ®) supplemented with 10% heat inactivated fetal bovine serum (FBS) (GIBCO ®), and 2mM 1-glutamine, 100 units/ml penicillin and 100 µg/ml streptomycin (GIBCO ®) at 37^0 C with a 5% CO_2/95% air atmosphere.

LGP2 wt (wt) and LGP2 knock out (LGP2-/-) mouse embryo fibroblasts (MEFs) derived from C57BL/6 mice were kindly provided by Dr. Michael Gale. MEFs were grown in DMEM (GIBCO ®) with 4500 mg/L glucose, sodium pyruvate and sodium bicarbonate supplemented with 10% heat inactivated fetal bovine serum (FBS) (GIBCO ®), and 2mM 1-glutamine, 100 units/ml penicillin and 100 µg/ml streptomycin (GIBCO ®) at 37^0 C with 5% CO_2/95% air atmosphere.

RNA interference

All siRNA duplexes were synthesized by Invitrogen and re-suspended in DEPC-treated water to a final storage concentration of 20µM. siRNA sequences used in the experiment are listed below (only one strand of each siRNA duplex is shown). The knockout efficiency of each siRNA duplex was examined by transfecting N terminal V5-

tagged full length LGP2 into A549 cells for 24 hours followed by siRNA treatment for 24 hours. Western blots were done using V5 antibody to determine efficiency of knockdown. Out of the three siRNA duplexes, oligo 2 (O2) and oligo 3 (O3) showed similar high efficiency of LGP2 knock down (more than 90% reduction of V5-tagged LGP2 protein expression in western blot analysis). O2 was chosen for subsequent experiments.

Sequences of siRNA used in the present study

siRNA	Sequence (sequence of complimentary strand not shown)
LGP2 (O1)	5′-CCCAACUUCUCGAACUACUAUAAUG
LGP2 (O2)	5′-CAACUGAAGGUAGCCGGGAGCUGAA
LGP2 (O3)	5′-GCCGGAAAUUUGGGACGCAAAUGUA

Confluent A549 cells were trypsinized, washed and re-suspended in serum and antibiotics-free Opti-MEM media at 3×10^5 cells per ml. 2.5 ml cell suspension was seeded into one well of a 6-well tissue culture plate immediately before siRNA transfection. For each siRNA transfection, Xtreme ® siRNA transfection reagent (Roche) was diluted with Opti-MEM I (Invitrogen) and incubated for 5 minutes. siRNA was mixed with Opti-MEM I and added to the diluted transfection reagent in a ratio of 2.5 µl reagent/20µM siRNA (final concentration) and the mixture was incubated at room temperature for an additional 25 minutes. The transfection complex was then added to

A549 cells and the plate was gently rocked to mix the cells and the transfection complex. The siRNA-transfected cells were incubated in serum and antibiotics-free Opti-MEM I (Invitrogen) for 24 hours at 37^0C. The culture medium was replaced with DMEM supplemented with 10% heat-inactivated FBS, 2mM L-glutamine, 100 units/ml penicillin and 100μg/ml streptomycin. Where indicated, cells were mock treated or infected with different strains of Influenza A virus.

Amplification of influenza A viruses

Recombinant influenza H3N2 A/Udorn/72 (Ud), G184R mutant Ud virus (G184R), H1N1 A/Texas/91 (Tx91), H1N1 A/California/09 (CA09), H5N1 A/Vietnam/04 (VN04), H3N2 A/Wisconsin/67/2005 (Wisc05) and H1N1 A/Brisbane/59/2007 (Bris07) virus stocks were amplified in 10-day old fertilized eggs and the virus titers were determined by plaque assays in MDCK cells. The VN04 virus was handled in a bio-safety level three laboratory (BSL-3).

Virus infection

For single-cycle virus infections, cells were infected with virus at a high multiplicity of infection (moi) of 5 plaque forming units (pfu)/cell. The cells were washed twice with PBS. Influenza virus was diluted in serum-free DMEM and added to the washed cells. After 1 hour of adsorption at 37^0C, cells were washed once with PBS and replenished with DMEM containing 2% FBS and incubated at 37^0C for indicated times. The supernatants and cell lysates were collected at indicated times.

Viral titer determination by plaque assay

MDCK cells were grown to confluency on 60 mm dishes. Prior to infection, the media was removed and cells were washed with PBS. Dilutions of influenza A viruses (in serum free DMEM) were added to the cells and allowed to adsorb for 1 hour at 37^0C. Cells were washed with PBS and serum-free DMEM containing a final concentration of 2.5μg/ml N-acetyl trypsin and 1% agarose was added. Once the agarose solidified, the plates were inverted and incubated at 37^0C for 2-3 days until the plaques started to appear. At the time of staining, the agarose was removed and the cells stained with naphthalene blue-black stain (1g naphthalene blue black powder, 60 ml glacial acetic acid, 13.6 g anhydrous sodium acetate in 1 liter distilled water) for 10 minutes at room temperature to count the plaques. The viral titer is calculated by the following formula:

Viral titer = number of plaques×dilution factor/volume of inoculum

Transfection/infection assays

The pOTB7 plasmid containing the cDNA for LGP2 was purchased from Thermo-scientific. The LGP2 cDNA was subcloned into a pcDNA3 vector that had been modified by inserting a V5 coding region adjacent to the CMV promoter, resulting in a cDNA encoding N-terminal V5-tagged LGP2. The cDNA sequence encoding the C-terminal repressor domain (RD) of LGP2 (amino acids 537-678) was also subcloned into the modified pcDNA3 vector, resulting in a cDNA encoding N-terminal V5-tagged LGP2 RD. The primers for making each construct are listed below. HeLa cells were transfected with either of these pcDNA3 vectors or an empty pCDNA3 control vector for 24 hours using the Mirus TransIT-1 transfection reagent, followed by infection with each of these viruses: Ud, Wisc05, Tx91 or Bris07 viruses for 6 or 9 hours. The amounts of full-length

LPG2 or the LGP2 RD expressed were determined using immunoblots probed with V5 antibody.

Sequences of primers used in the present study

Primer name	**Sequence of primer**
Cloning of FL LGP2	
BglII Forward	5′ GGAAGATCTATGGAGCTTCGGTCCTACCA 3′
EcoRI Reverse	5′ CCGGAATTCTCAGTCCAGGGAGAGGTCCGAC 3′
Internal Reverse	5′ GCATCTCCAGTTTTGGAATTCTCTGG 3′
Internal Forward	5′ CTGTGTGCCGAGCGCCGGCTGCTGG 3′
Cloning of RD LGP2	
BglII Forward RD	5′GGAAGATCTATGGCAGCCCAGCGGGAGAACCA 3′

RNA assays

After the appropriate treatment, the culture medium was removed and the cells were washed once with PBS. Cells were then lysed, and total RNA was extracted with Trizol reagent (Invitrogen) according to manufacturer's instructions. Where indicated, the RNA from infected cells was reverse transcribed using oligo dT to measure the level of mature IFN-β mRNA, β-actin mRNA and HPRT mRNA (house-keeping gene). Reverse transcription was performed using Transcriptor First Strand cDNA synthesis Kit (Roche) in a 20μl reaction mixture. To measure the level of IFN-β pre-mRNA in infected cells, 1 μg of total RNA, which corresponds to equal cell equivalents was reverse-transcribed using a 20-mer oligonucleotide (5′CAACTAATAGGTACTTGG CA 3′) complementary

to a sequence 76-95 bases downstream from the poly(A) addition site of human IFN-β pre-mRNA as previously described (Kuo, Zhao et al. 2010).

The amounts of both IFN β pre-mRNA and IFN-β mRNA were determined using the Taqman gene expression assay (Applied biosystems) with 5′ and 3′ primers complementary to internal sequences shared by the pre-mRNA and mRNA (forward 5′-CAGTCTGCACCTGAAAAATATTATG-3′; reverse 5′-GATTTCCACTCTGACTATGGTCCAGG-3′) and a Taqman MGB (minor groove binder) internal probe. Taqman gene expression assays from Applied Biosystems were used to determine the amounts of IFN pre-mRNA, IFN-mRNA, β-actin and mouse HPRT mRNA. Real-time PCR analysis was carried out using the Perkin-Elmer/Applied Biosystems 7900HT sequence detector. The quantitative PCR reaction for each sample was performed in triplicate. Error bars are shown in each figure.

For Northern blot analysis, 10μg total RNA/sample was separated on 1.2% agarose gel. RNA was then transferred and UV-crosslinked onto nylon membrane (Nytran ®, Whatman Schleicher & Schuell). To prepare the ^{32} P-labeled probes for ISG56/p56, the PCR product of full-length ISG56 was used as template for the random priming reaction. Random primers were produced by Klenow fragment in the presence of α-^{32} P-dCTP using RadPrimer ® DNA labeling system (Invitrogen). Unincorporated nucleotides were removed by using ProbeQuant 50 (GE Healthcare). After hybridization, signal strength was determined by scanning the activated phosphor imaging screen (Bio-Rad) with Typhoon Trio (GE Healthcare) and analyzed by ImageQuant software.

Immunoblots

For the assays for activated (phosphorylated) IRF3 and STAT1, cells at the indicated times after infection were suspended in the PhosphoSafe extraction reagent (Novagen). After vortexing, the mixture was maintained at 4^0C for 10 minutes and then centrifuged at 10,000g for 5 minutes. An aliquot of the supernatant was subjected to SDS-polyacrylamide gel electrophoresis (PAGE), followed by immunoblots using an antibody against either (serine 396-phosphorylated) IRF3 or (tyrosine 701-phosphorylated) STAT1 (Cell Signaling). For the assays for other proteins, cells collected at the indicated times after infection were lysed in RIPA buffer (50mM Tris-HCl pH 7.5, 150mM NaCl, 1% NP-40, 0.5% sodium deoxycholate, 0.1% SDS) supplemented with Complete ® protease inhibitor (Roche). Immunoblots were probed using antibodies against the viral NS1 protein, LGP2 (IBL-America), or β-tubulin (Cell Signaling). Antibodies against the major structural protein of influenza A/Udorn/72 virus which detects the HA, NP and M1 (matrix) proteins was kindly provided by Dr. Robert A. Lamb (Northwestern University).

Proteins were separated by SDS-PAGE (12% gel) and transferred onto nitrocellulose membrane (Bio-Rad) by a semi-dry transfer method (0.8 mA/cm^2). Blots were blocked in TBS containing 0.2% Tween (TBST) and 5% non-fat dried milk at room temperature for 1 hour and then incubated with primary antibodies at 4^0C overnight. The blots were washed three times with 0.2% TBST. Secondary antibodies, rabbit anti-mouse IgG HRP (Santa Cruz), anti-rabbit IgG HRP (GE Amersham) or donkey anti-goat IgG HRP (Santa Cruz) were diluted (1:10000) in blocking buffer. Membranes were incubated with these diluted secondary antibodies for an hour at room temperature and washed four

times with TBST. Proteins were detected with enhanced chemiluminescence (ECL) western blotting substrate (Pierce) and exposed to CL-exposure film (Pierce).

Expression microarray analysis

A549, HeL299 and GRE cells were infected with different viruses as indicated. All virus infections were done at a high moi of 5. After indicated times postinfection, total RNA was isolated using Trizol ® reagent according to manufacturer's protocol. RNAs from virus infected cells and mock treated cells were used for comparative microarray analysis. NimbleGen *Homo sapiens* 12 plex microarrays were used with duplicate arrays for each sample. Ten micrograms of total RNA were processed and labeled following the standard NimbleGen protocol. RNA was converted into cDNA using the SuperScript II cDNA conversion kit (Invitrogen). Double-stranded cDNA was random-prime labeled with Cy3-nonamers and hybridized to the microarrays for 16 hours at 42^0C. The arrays were washed, dried and scanned at 5μM resolution using a GenePix 4000B microarray scanner (Molecular Devices, Sunnyvale, CA). Data were extracted from scanned images using Nimblescan 2.2 version 5 software (Roche, Nimblegen). Briefly Tiff images of the hybridized chips were obtained and the data were normalized using the Quantile Normalization and Robust Multiarray Averaging (RMA) analysis tool in the Nimblescan 2.2 version 5 software package. The normalized data were then imported into Arraystar software for further analysis. The mean of the duplicate data was determined for each pair of arrays. The fold change in virus infected samples was then determined relative to that of the mock infected samples. The data from the replicate arrays for each RNA sample showed minimal difference (R^2>0.95). Consequently the

fold changes for individual mRNA showed minimal differences between the two replicate arrays. Messenger RNAs from the data set that met the twofold change cutoff were loaded into the DAVID webserver (http://david.abcc.ncifcrf.gov/) and search parameters were set to include all available categories from the three gene ontologies (GOs): biological process, cellular component and molecular function. This program uses the Fisher exact test to determine significance.

Enzyme linked immunosorbent assays (ELISAs)

Culture supernatants were collected after virus infection as indicated and the cytokine concentrations were measured using ELISA kits for mouse IFN-β (PBL Biomedical Laboratories) according to manufacturer's instructions.

2.3 RESULTS

2.3.1 LGP2 is induced during influenza A virus infection

The NS1 protein binds to the 30kDa subunit of cleavage and polyadenylation specificity factor (CPSF) and inhibits 3′ end processing of cellular transcripts (Das, Ma et al. 2008; Kim, Latham et al., 2002; Nemeroff, Barabino et al. 1998; Noah, Twu et al. 2003). Since our goal was to identify transcripts that were up or downregulated during virus infection, we used a mutant Ud virus, G184R. The NS1 protein of this virus has a mutation at position 184 from G to R and as a result it does not bind to the 30kDa subunit of CPSF. Therefore, cellular pre-mRNA processing is no longer inhibited by the NS1 protein and the pre-mRNAs are efficiently processed into mature mRNAs in the

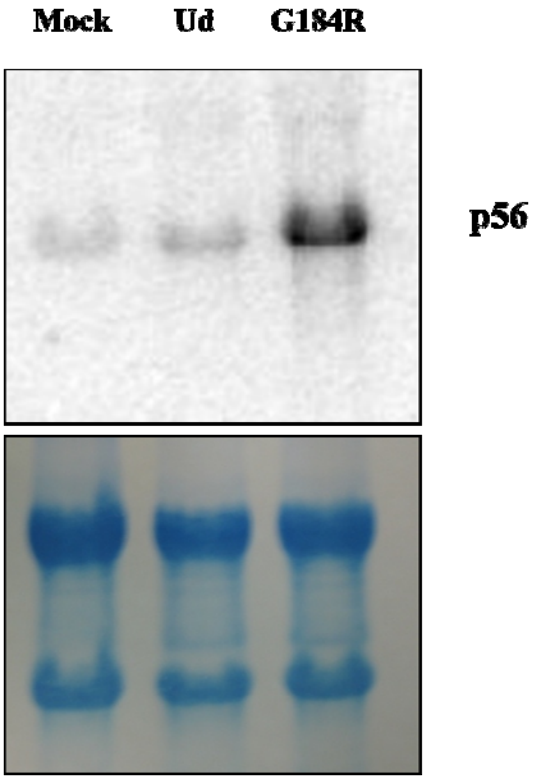

Figure 2.1 p56 induction in Ud and G184R-virus infected cells
Total RNAs extracted from GRE cells infected with Ud and G184R mutant virus were subjected to Northern blot analyses to detect expression of ISG56 or p56 mRNA. The lower panel is a coomassie stain to show equal loading in all lanes.

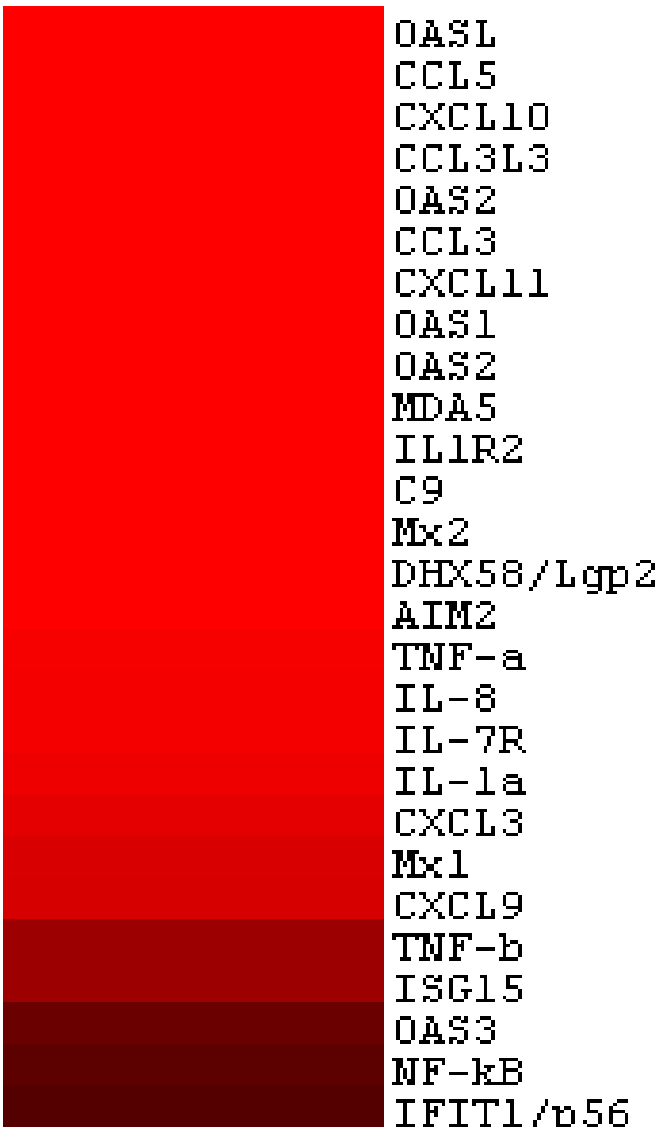

Figure 2.2 LGP2 is upregulated in influenza A virus infected cells.
Heat map showing gene expression changes in G184R virus infected-cells relative to mock-treated cells and LGP2 induction after hybridization onto Nimblegen *Homo sapiens* microarray chips

Cell type (Human)	Virus strain	Lgp2 mRNA relative to Mock (Fold change)	
GRE (Brain)	G184R (H3N2)	+14	→ Microarray
A549 (Lung)	Ud WT (H3N2)	+12	→ qPCR
	G184R (H3N2)	+16	
	CA09 (H1N1)	+15	
Hel299 (Lung)	Ud WT (H3N2)	+9	→ Microarray+qPCR
	CA09 (H1N1)	+8	
	VN04 (H5N1)	+10	

Table 2.1 LGP2 is induced after infection with H3N2, H1N1 and H5N1 virus subtypes

cytoplasm. When total RNAs extracted from GRE cells infected with either Ud or G184R virus were subjected to Northern blot analyses, there was significantly more ISG56/p56 expression in the G184R virus-infected cells compared to the Ud virus-infected cells (Figure 2.1). Based on this result, using microarrays, we extended our study to a genome-wide scale in order to identify other transcripts like p56 that might be up or downregulated after virus infection.

We identified LGP2 as a virus-induced transcript when we compared the expression profiles of G184R virus-infected GRE cells to mock treated cells (Figure 2.2). In this analysis, there were several transcripts that were upregulated specifically in the "defense response related genes" category based on analysis using DAVID. A subset of the upregulated transcripts from that category is shown in a heat map (Figure 2.2). These included several cytokines and chemokines like CCL5, CXCL10, CCL3, CXCL11, IL-8, IL-1a, CXCL3, CXCL9 and TNF-β. A number of transcripts encoding antiviral proteins such as ISG15, p56, OAS1, OAS2, Mx1 and Mx2 were also upregulated. LGP2 also known as DHX58 was 14 fold upregulated in virus-infected cells. The induction of LGP2 was observed after infection in other cells like A549, HeL299 and HeLa. The different subtypes of viruses that induced LGP2 include H3N2s (Ud, G184R), H1N1s (CA09, Tx91) and H5N1 (VN04) (Table 2.1).

2.3.2 The role of LPG2 in influenza A virus-infected mouse embryo fibroblasts

As one approach to assess the role of LGP2 in influenza A virus infection, we infected wt and LGP2-/- mouse embryo fibroblasts (MEFs) with the H3N2 Ud virus or

the H1N1 Tx91 virus, and determined the amount of IFN-β mRNA produced at various times after infection using quantitative RT-PCR. First, LGP2 mRNA was measured by reverse transcription-PCR (RT-PCR) in LGP2-/- and wt MEFs. There was no LGP2 detected in LGP2-/- MEFs whereas LGP2 was induced in the wt MEFs confirming that the LGP2-/- or knockout MEFs lacked the LGP2 gene (Figure 2.3 A). The amount of IFN-β mRNA produced in Ud virus-infected LGP2-/- MEFs was greater than that produced in wt MEFs and the magnitude of this difference increased with times post-infection, from only 20% higher at 3 hours to 400-500% higher at 12 hours after infection. These results demonstrate that LGP2 substantially downregulates the production of IFN-β mRNA in MEFs infected with H3N2 Ud virus (Figure 2.3 B, left panel).

The IFN-β mRNAs produced in H3N2 Ud-virus infected MEFs are derived from pre-mRNAs that have escaped the inhibition of their 3′ end processing resulting from the binding of the NS1 protein to CPSF30. Because little or no NS1 protein was detected at 3 hours postinfection (Figure 2.3 B, lower panel: western blot), minimal inhibition of the 3′ end processing of IFN-β pre-mRNA would be expected to occur, accounting for the production of IFN-β mRNA in both wt and LGP2-/- MEFs at 3 hours post-infection. At later times after infection the amount of IFN-β mRNA did not increase in wt-infected MEFs, but did increase in infected LGP2-/- MEFs, resulting in the 4-5-fold higher level of IFN-β mRNA in LGP2-/-infected MEFs at 12 hours after infection. This increase is attributable to increased transcription of the IFN-β gene, due at least in part to increased

A

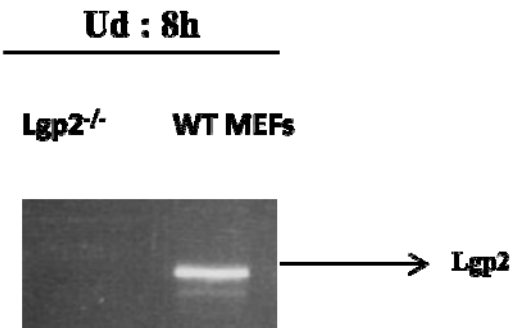

B

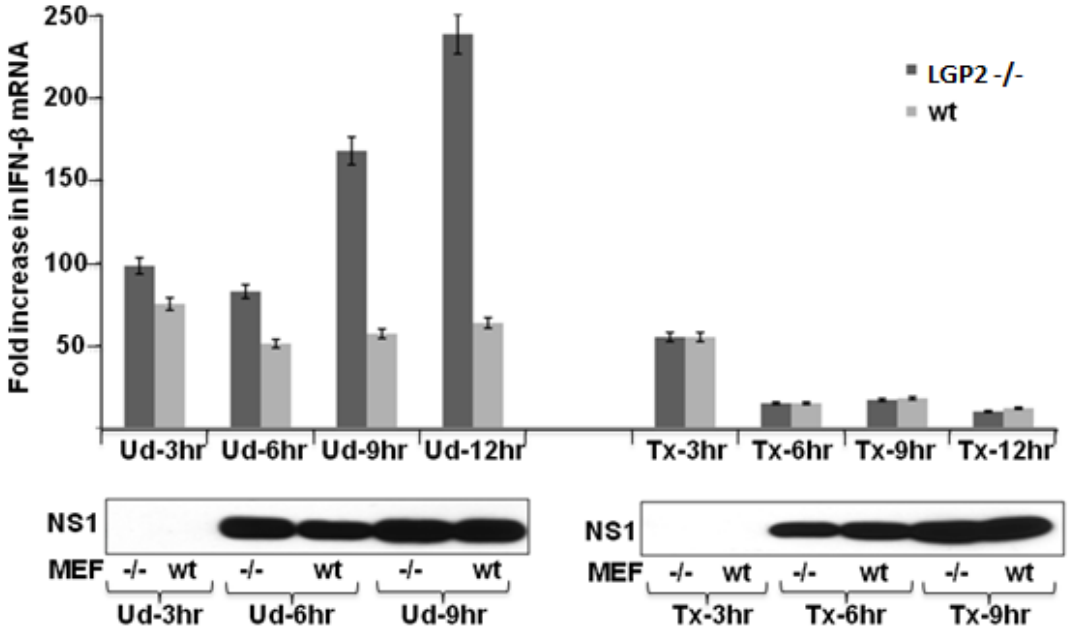

Figure 2.3 LGP2 plays a negative role in Ud virus infected MEFs.
A. RT-PCR was performed to measure LGP2 mRNA production in wt and LGP2-/- MEFs after Ud virus infection. B Upper panel: qPCR was performed to measure IFN-β mRNA in mouse cells after Ud and Tx91 virus infection. Lower panel: wt and LGP2-/- MEFs were infected with Ud and Tx91 virus and western blotting was done to detect NS1 protein levels after virus infection

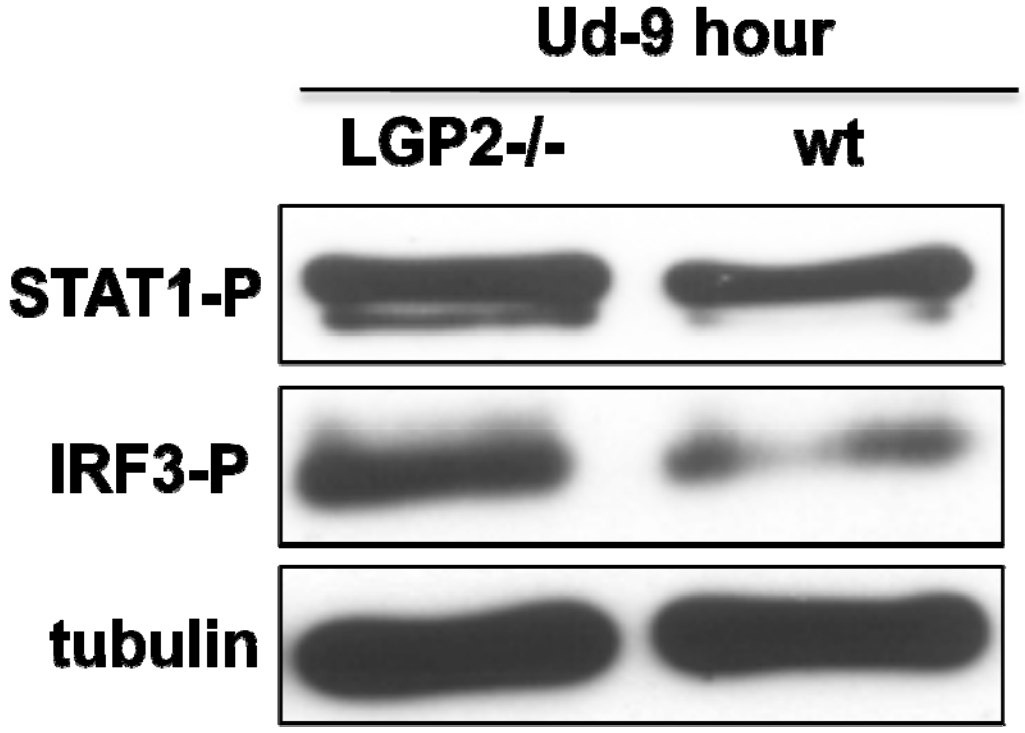

Figure 2.4 LGP2 inhibits innate immune signaling after Ud virus infection in MEFs. wt and LGP2-/- MEFs were infected with Ud virus for 9 hours. Lysates were prepared and western blotting was done to detect the level of STAT1 and IRF3 activation

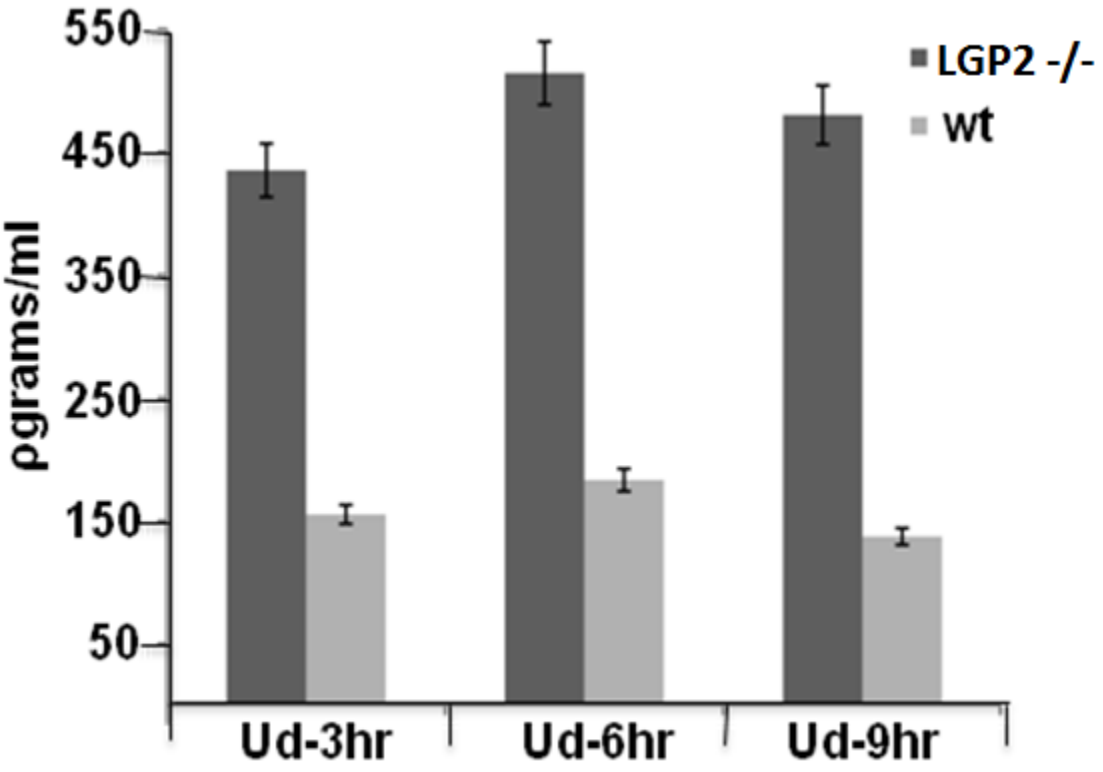

Figure 2.5 Time course of IFN-β protein expression after virus infection in MEFs. wt and LGP2-/- MEFs were infected with Ud virus at an moi of 5 for 3, 6 and 9 hours. Cell culture supernatants were collected at different times and the amount of IFN-β protein was measured by ELISA.

activation of IRF3 that was observed (Figure 2.4). The increase in IFN-β mRNA resulted in an increase in secreted IFN-β detected by ELISA (Figure 2.5), and an increase in the activation of the STAT1 transcription factor that is induced by IFN-β (Figure 2.4).

In contrast, the same amount of IFN-β mRNA was produced in H1N1 Tx91 virus-infected wt and LGP2-/- MEFs (Figure 2.3 B, right panel). The production of some IFN-β mRNA in both wt and LGP2-/- MEFs at 3 hours post-infection presumably occurred because little or no NS1 protein was produced by 3 hours after infection. No increase in IFN-β mRNA was detected at later times in either wt or LGP2-/- virus-infected MEFs (Figure 2.3B), and little or no IFN-β protein was detected by ELISA (data not shown). Consequently, we did not detect any role for LGP2 in MEFs infected with the H1N1 Tx91 virus.

2.3.3 The role of LGP2 in influenza A virus-infected human cells

We first established that the LGP2 protein is synthesized in A549 cells and HeLa cells (data not shown), indicating that LGP2 mRNA is also constitutively synthesized. Infection with either the Ud or Tx91 virus induced similar increases in LGP2 mRNA (approximately 8-fold) (Figure 2.6 A) and in LGP2 protein (approximately 5-fold) (Figure 2.6 B). Because the Tx91 virus does not activate IRF3, these results suggest that the transcription of the LGP2 gene does not require activated IRF3.

The H3N2 Ud and H1N1 Tx91 viruses have dramatically different effects on the cellular innate immunity pathway (Figure 2.7). We measured the production of IFN by

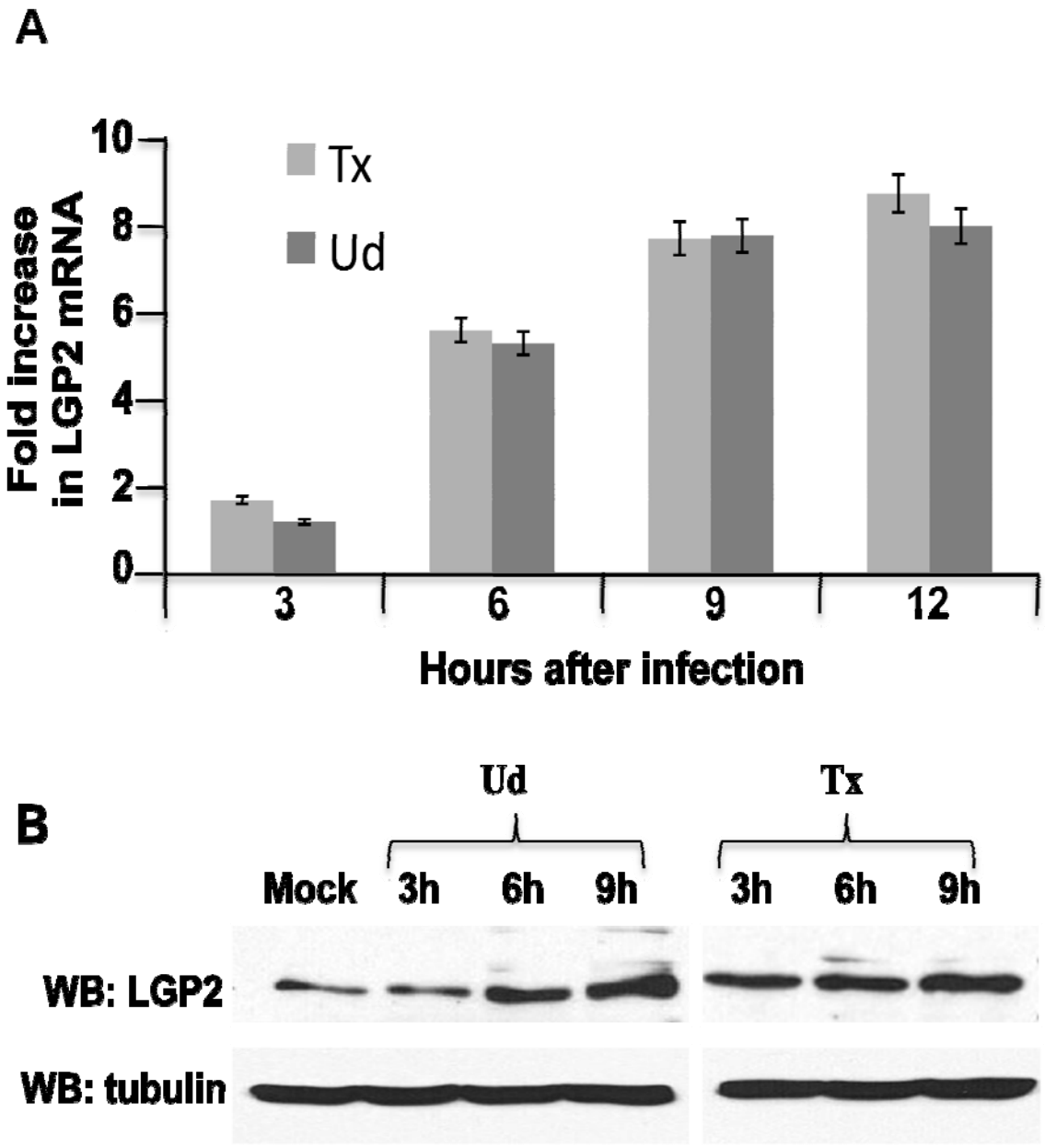

Figure 2.6 LGP2 is induced after infection with Ud and Tx91 viruses.
A. Total RNA was collected and qPCR was done to detect LGP2 mRNA levels after Tx91 and Ud virus infection B. Western blots were prepared to measure LGP2 protein induction after virus infection over time.

assaying for activation (phosphorylation) of STAT1, the transcription factor activated by IFN (Figure 2.7, left panels). STAT1 was strongly activated in Ud virus-infected HeLa cells at 3 and 6 hours after infection. In fact, detectable STAT1 activation preceded the detection of IRF3 activation, presumably because the STAT1-P antibody works better than the IRF3-P antibody in immunoblots. The synthesis of the NS1 protein was detected starting at 6 hours after infection and the amount of the NS1 protein substantially increased at later times (9 and 12 hours). Concomitant with the increase in the amount of the NS1 protein, the level of STAT1 activation decreased, most likely because the increased levels of the NS1 protein effectively inhibited the 3′ end processing of IFN pre-mRNA. In contrast, in Tx91 virus-infected cells little or no activation of either STAT1 or IRF3 was detected (Figure 2.7, right panels), even though the time course of NS1 protein synthesis was similar to that in Ud virus-infected cells.

We undertook two ways to determine the role of LGP2 in human cells infected with influenza A viruses (i) siRNA knockdown and (ii) overexpression of LGP2.

LGP2 is efficiently knocked down in transfection experiments in tissue culture

We used siRNA against LGP2 to deplete LGP2 message. The experimental design for the knockdown experiments is shown in Figure 2.8 A. Since we wanted to determine the efficiency of knockdown, LGP2 expressing a V5 tag was used because at that time an antibody that recognizes LGP2 was unavailable. A549 cells were transfected with V5-LGP2 for 24 hours. After 24 hours, the cells were treated with the following siRNAs for an additional 24 hours-O1, O2 or O3, all specific for LGP2 or a scrambled

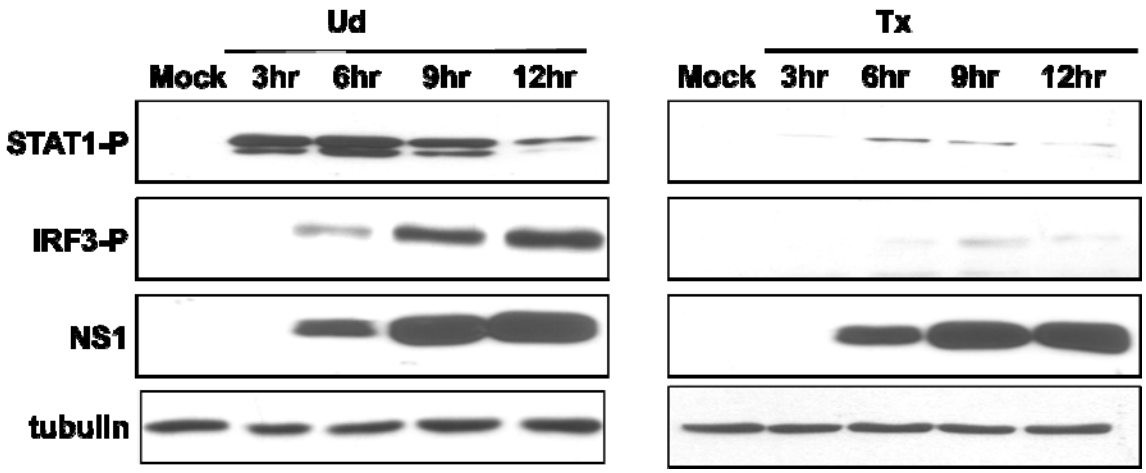

Figure 2.7 Ud (H3N2) and Tx91(H1N1) viruses have dramatically different effects on innate immune signaling.
HeLa cells were infected with Ud virus or Tx91 virus. Lysates were prepared and subjected to western blotting to detect activated STAT1, activated IRF3 and NS1 protein expression in Ud virus-infected cells (Left panels) and Tx91 virus infected cells (Right panels).

control siRNA (CTRL). Cell lysates were prepared and blotted using V5 antibody. The western blot showed that the O2 and O3 siRNAs were able to efficiently knockdownV5-LGP2 expression compared to CTRL siRNA (Figure 2.8 B). O1 was not efficient in knockdown of V5-LGP2 expression and was not used for subsequent experiments. Therefore, we identified two siRNAs that effectively inhibited the synthesis of LGP2 mRNA and protein when they were transfected for 24 hours with a plasmid expressing LGP2.

LGP2 is not efficiently knocked down after virus infection

In order to understand the role of LGP2 during virus infection, we designed an experiment wherein A549 cells were transfected with O2 siRNA or CTRL siRNA for 24 hours. After 24 hours, cells were infected with H3N2 Ud virus (Figure 2.9 A). RNA was extracted with Trizol, and LGP2 mRNA levels were measured by qPCR to determine the efficiency of knockdown. Although, we identified siRNAs that can efficiently knock down LGP2 expression in transfection experiments (Figure 2.8), the knockdown efficiency was only 50-60% in virus infected cells (Figure 2.9 B). More importantly, LGP2 protein was still detectable after siRNA treatment with O2 in virus infected cells (Figure 2.9 C). Since many other protocols failed to achieve knockdown, we focused on LGP2 overexpression to study its effect on the interferon response.

2.3.4 Effect of LGP2 overexpression on the influenza virus-induced antiviral response

In our second approach we transfected a LGP2 expressing plasmid into HeLa cells for 24 hours and determined how the overexpression of LGP2 affects the influenza virus-induced antiviral response. We measured the activation of two important transcription factors: IRF3 and STAT1. IRF3 is activated through the RIG-I pathway and once activated it translocates to the nucleus and drives transcription of the IFN-β gene. Once IFN-β protein is synthesized, it signals in an autocrine or paracrine manner to activate the JAK-STAT pathway, which then induces hundreds of ISGs leading to the establishment of an antiviral state in the host. Therefore measuring activated IRF3 and STAT1 assays the production of functional IFN molecules.

HeLa cells were transfected for 24 hours with a plasmid expressing either full-length LGP2 or the LGP2 RD (RD) (Figure 2.10 A), or as a control an empty plasmid, followed by infection with the H3N2 Ud virus for 6 hours (Figure 2.10 B). Overexpression of LPG2 or its RD domain suppressed the antiviral response induced by the H3N2 Ud virus. STAT1 activation was reduced approximately 10-fold, as determined by an immunoblot (Figure 2.10 B), reflecting a similar 10-fold reduction in the production of both IFN-β pre-mRNA and IFN-β mRNA, as measured by quantitative RT-PCR (Figure 2.11). The latter results also document the strong inhibition of the 3′ end processing of IFN-β pre-mRNA by the NS1 protein at 6 hours after infection: the amount of IFN-β mRNA was only 10-15% the amount of IFN-β pre-mRNA.

A

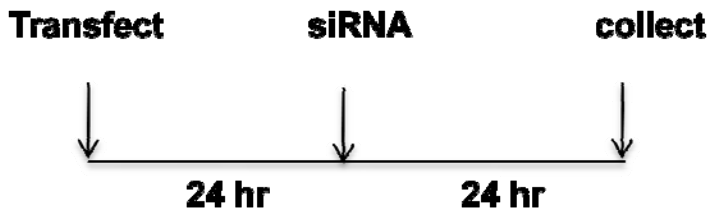

B

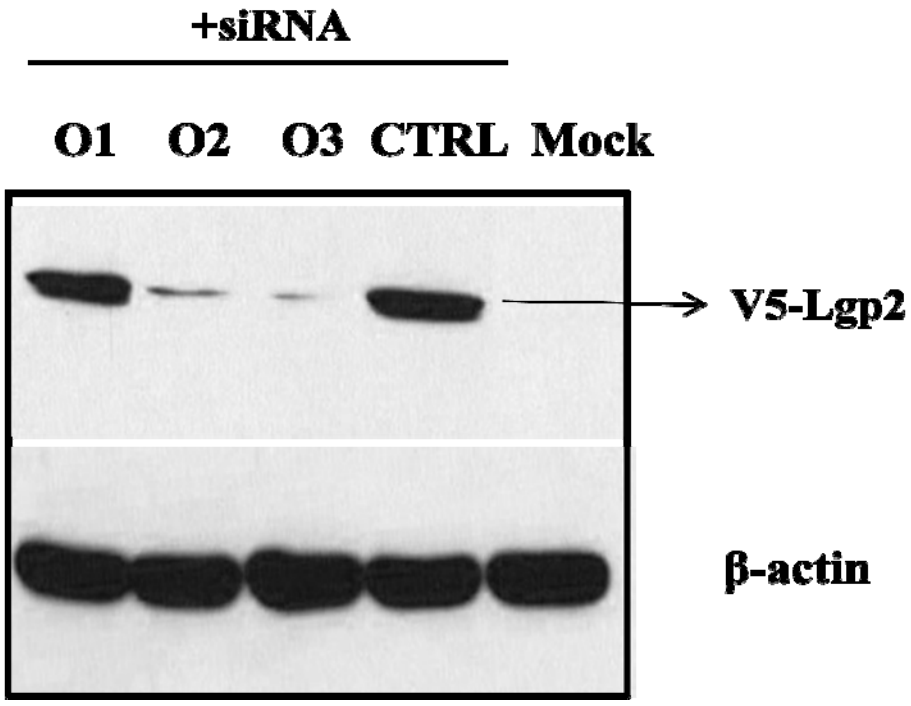

Figure 2.8 LGP2 is efficiently knocked down in transfection experiments.
A. A549 cells were transfected with V5-LGP2 for 24 hours. After 24 hours, the cells were treated with siRNAs O1, O2, O3 that act against LGP2 or a control siRNA as shown in the schematic. B. Western blot analysis of cell lysates using V5 antibody to measure efficiency of siRNA treatment.

A

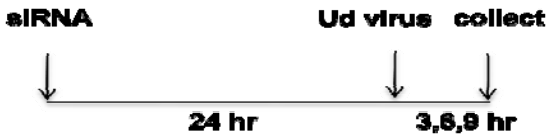

B

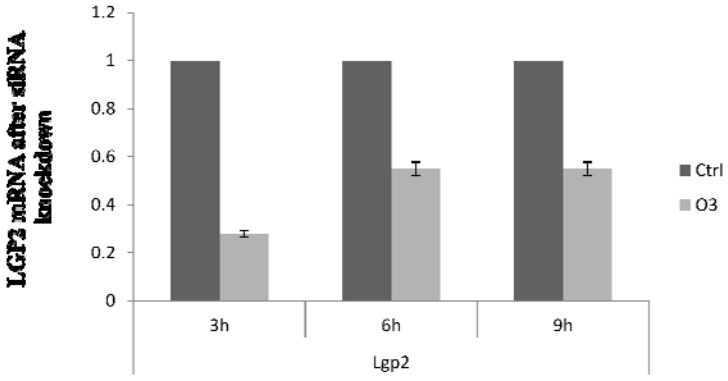

C

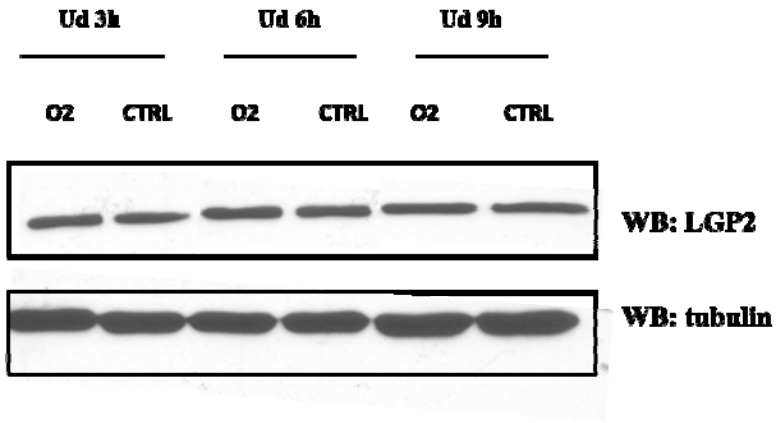

Figure 2.9 LGP2 is not efficiently knocked down after virus infection.
A. A549 cells were siRNA treated for 24 hours and infected with Ud virus for 3, 6 and 9 hours as shown in the schematic. B. qPCR was performed to measure the knockdown efficiency of siRNA treatment by measuring LGP2 mRNA levels C. Western blotting using anti-LGP2 antibody was done to measure level of LGP2 protein in control (CTRL) and O2 siRNA treated cells.

The reduction in IRF3 activation, as determined by an immunoblot was smaller, approximately 2-4-fold. These results demonstrate that LPG2 downregulates the antiviral response and the production of IFN in cells infected by the H3N2 Ud virus. In contrast, LPG2 overexpression had no detectable effect on the antiviral response induced by the H1N1 Tx91 virus (data not shown), because the antiviral response, e.g., STAT1 and IRF3 activation, was already so minimal in the absence of LGP2 overexpression (Figure 2.7, right panels). To establish whether the above effects of LGP2 are shared by other H3N2 and H1N1 viruses, we carried out LGP2 overexpression experiments with other H3N2 and H1N1 viruses. As seen in Figure 2.12, overexpression of LGP2 caused approximately a 10-fold reduction in the STAT1 activation induced by the H3N2 Wisc05 virus (left panel), verifying that LGP2 downregulates IFN production in H3N2 virus-infected cells. In contrast, because the H1N1 Bris07 virus did not induce detectable activation of STAT1, no effect of LGP2 overexpression on STAT1 activation was detected (Figure 2.12, right panels).

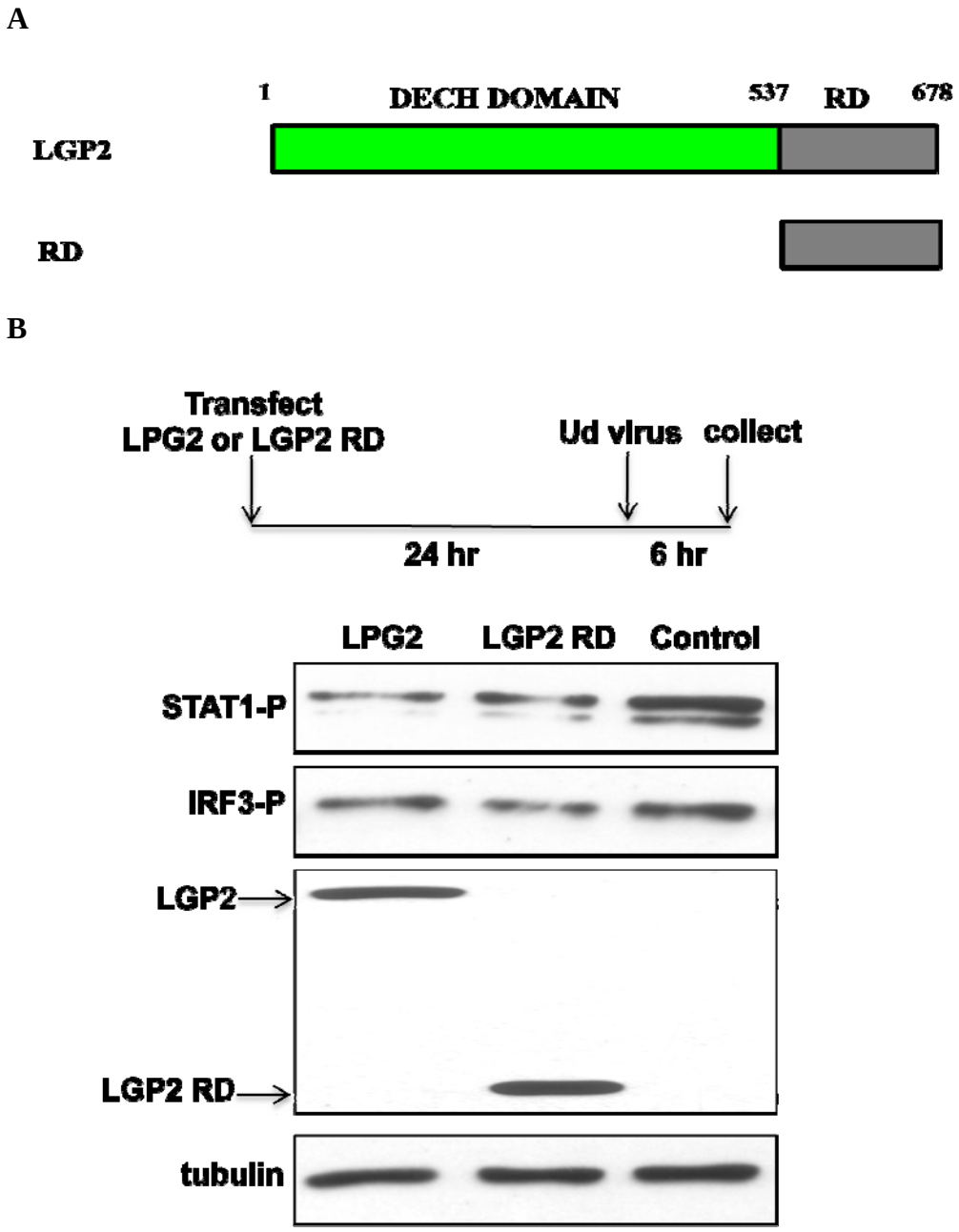

Figure 2.10 LGP2 inhibits STAT1 activation in human cells infected with Ud virus. A. Schematic of the two constructs, full length LGP2 (1-678) and the repressor domain (RD) only (537-678 amino acids) used in this study are shown. B. HeLa cells were transfected with LGP2, RD or Control plasmid for 24 hours followed by Ud virus infection for 6 hours. Cell lysates were prepared and levels of STAT1 and IRF3 activation was measured by western blotting. Both LGP2 and RD were expressed at similar levels.

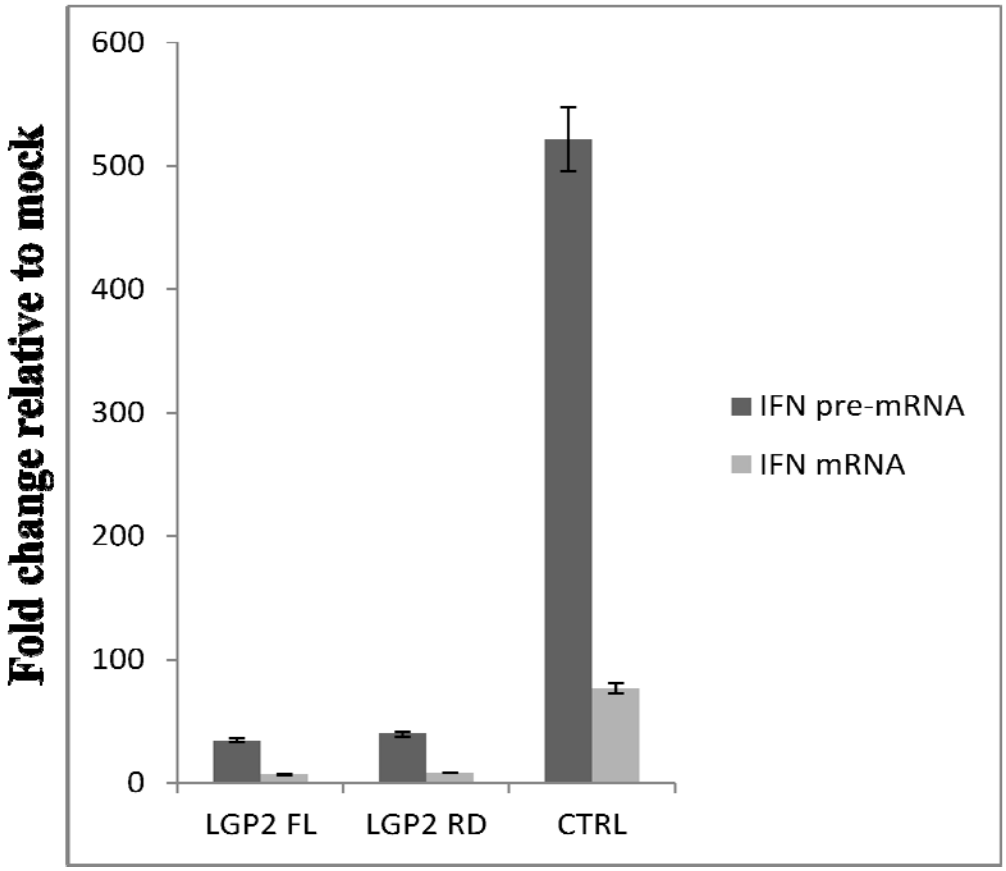

Figure 2.11 Expression of LGP2 or RD results in suppression of IFN pre-mRNA and IFN mRNA production.

HeLa cells were transfected with LGP2, RD or Control plasmid for 24 hours followed by Ud virus infection for 6 hours. RNA was extracted from the cells and the level of IFN-β pre-mRNA and IFN-β mRNA was measured by qPCR.

A

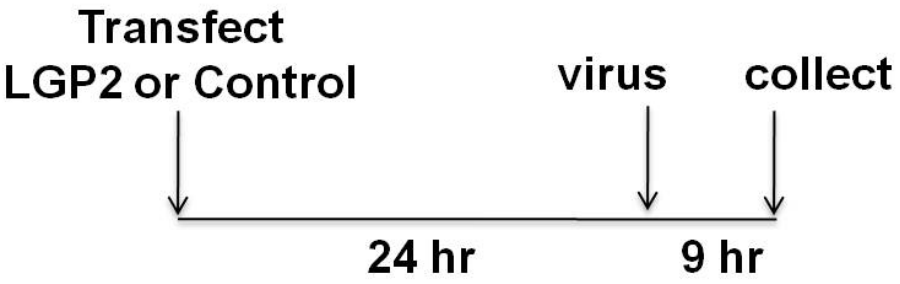

B

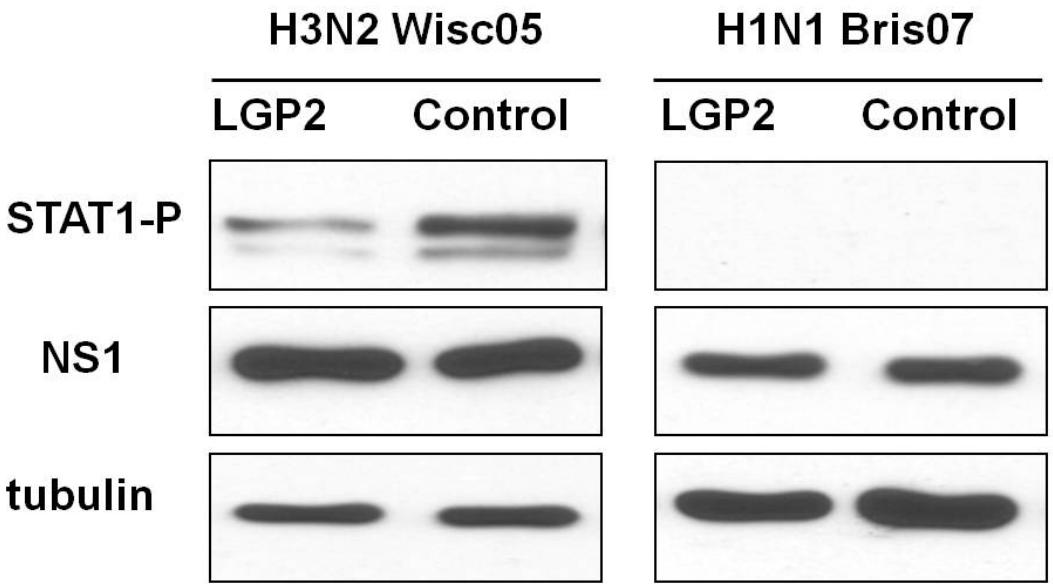

Figure 2.12 LGP2 inhibits STAT1 activation in human cells infected with Wisc05 virus.

A. HeLa cells were transfected with LGP2 or Control plasmid for 24 hours followed by infection with H3N2 Wisc05 virus (B, left panel) or H1N1 Bris07 virus (B, right panel) for 9 hours. Western blotting was done to detect the level of activated STAT1 after virus infection.

2.4 DISCUSSION

RIG-I and MDA5 belong to the RLR family and are important in innate immunity. They act as pattern recognition receptors (PRRs) capable of sensing virus infection and triggering the IFN response. LGP2 is the third member of the RLR family of receptors. The role of LGP2 in RLR signaling and the IFN response has been controversial. In the current study we show that LGP2 is induced by different subtypes of influenza A viruses (H3N2, H1N1 and H5N1). We establish that LGP2 downregulates the production of IFN in mouse and human cells infected by wild-type H3N2 influenza A viruses, which encode NS1 proteins that do not block the activation of IRF3 and IFN-β transcription. The extent of this downregulation was determined using wt and LGP2-/- mouse cells: endogenous LGP2 decreased IFN production 3-4-fold. We presume that endogenous LGP2 causes a similar reduction in IFN in human cells, in light of our demonstration that LGP2 overexpression decreased STAT1 activation and IFN-β transcription approximately 10-fold. Consequently, our results demonstrate that LGP2 negatively affects the RIG-I-mediated activation of IFN transcription in cells infected with wild-type H3N2 influenza A viruses. One or more of the mechanisms that have been proposed for the LPG2-mediated inhibition of RIG-I signaling likely operate in cells infected by H3N2 influenza A viruses (reviewed in Vitour and Meurs, 2007).

In cells infected by circulating H3N2 influenza A viruses, IRF3 and IFN transcription are activated, but the production of mature IFN mRNA is inhibited because the viral NS1 protein binds CPSF30, thereby inhibiting the 3′-end processing of IFN pre-

mRNA. However, as further documented here, significant levels of IFN mRNA are produced at early times after infection (3-6 hours postinfection) prior to the time at which the NS1 protein is synthesized in sufficient amounts to efficiently block the 3′ end processing of IFN pre-mRNA. During this early time, the production of IFN is downregulated only by LGP2 (Figure 2.3 B). At later times, IFN production is downregulated by both LGP2 and the NS1 protein-mediated inhibition of IFN pre-mRNA processing. These results raise the possibility that downregulation of IFN production by LGP2 may be important, if not necessary, for the appropriate regulation of IFN production that enables H3N2 influenza A viruses to replicate efficiently.

IFN transcription and the production of IFN are induced by wild-type H3N2 viruses and also by an attenuated H1N1 PR8 virus that does not encode a NS1 protein. However, the effects of LPG2 on IFN production induced by these two viruses are strikingly different. As shown here, LGP2 downregulates IFN production induced by wild-type H3N2 viruses, whereas it has been reported that LGP2 has no effect on the production of IFN induced by the attenuated PR8 virus (Satoh, Kato et al. 2010). Consequently, there is at least one important difference in the RIG-I signaling pathways induced by the wild-type H3N2 viruses and the attenuated PR8 virus that does not encode a NS1 protein.

Currently circulating H1N1 viruses via their NS1 proteins effectively inhibit the RIG-I-mediated activation of IRF3 and the production of IFN (Kuo, Zhao et al. 2010). It is therefore not surprising that further downregulation of this RIG-I pathway by LGP2 cannot be detected. Our results thus provide another way that the regulation of IFN

production in H1N1 influenza A virus-infected cells differs from the regulation in H3N2 influenza A virus-infected cells. In summary, my research has led to the identification of a virus-induced transcript, LGP2 that plays a negative role in RIG-I mediated signaling in H3N2 Influenza A virus-infected cells. This is the first instance wherein the role of LGP2 has been described in naturally occurring, non-attenuated influenza A viruses. Further studies *in vivo* will be necessary to determine whether the negative role of LGP2 in RIG-I signaling has any impact on adaptive immunity.

CHAPTER 3: THE VIRULENCE OF 1997 H5N1 INFLUENZA VIRUSES IN THE MOUSE MODEL IS INCREASED BY CORRECTING A DEFECT IN THEIR NS1 PROTEINS

3.1 INTRODUCTION

Highly pathogenic H5N1 influenza A viruses were first transmitted from chickens to humans in 1997 in Hong Kong (Claas, Osterhaus et al. 1998; Subbarao, Klimov et al. 1998). Following culling of the poultry in Hong Kong, subsequent transmission of H5N1 viruses to humans was not documented until 2003 (Guan, Poon et al 2004; Peiris, Yu et al. 2004). Since then, H5N1 influenza viruses have spread from Asia to Africa and Europe, resulting in more than 500 human infections with a case fatality rate of approximately 60% (Chen, Bright et al. 2007; Kandun, Tresnaningsih et al. 2008; Sedyaningsih, Isfandari et al. 2007; Wang, Zhao et al. 2010). Fortunately, H5N1 viruses have not yet acquired the ability for efficient poultry-to-human and human-to-human transmission (Uyeki and Breesee 2007; Vong, Coghlan et al. 2006), but the possibility of efficient human-to-human transmission coupled with high virulence makes these viruses a major public health concern.

The molecular basis for the high virulence of H5N1 viruses that have infected humans remains unclear (Gambotto, Barratt-Boyes et al. 2008; Hatta, Hershberger et al. 2010). The presence of multiple basic amino acids adjacent to the hemagglutinin (HA) cleavage site is crucial for virulence because these amino acids allow the HA to be cleaved by ubiquitous intracellular furin-like proteases (Hatta, Hershberger et al. 2010; Horimoto and Kawaoka 1994). However, the presence of such a HA cleavage site is not

sufficient for lethality in mammalian hosts. Therefore, it is of great importance to identify specific functions of other viral proteins that play critical roles in virulence for humans. Both structural and non-structural gene products have been reported to contribute to the enhanced replications and virulence of H5N1 in mammalian animal models (Chen, Bright et al. 2007; Naffakh, Tomoiu et al. 2008; Seo, Hoffmann et al. 2002).

The NS1 protein plays a major role in countering the innate immune response to influenza viral infection, largely by preventing the interferon response through at least two mechanisms. In one mechanism, the NS1 protein inhibits the activation of the IRF3 transcription factor, thereby inhibiting the activation of interferon beta (IFN-β) gene transcription and hence the synthesis of IFN-β pre-mRNAs (Chen, Bright et al. 2007; Mibayashi, Martínez-Sobrido et al. 2007; Pichlmair, Schulz et al. 2006; Talon, Horvath et al. 2000; Wang, Riedel et al. 1999). Influenza A strains that circulate in humans differ markedly in the abilities of their NS1 proteins to inhibit the activation of IRF3 and IFN-β transcription. For instance, the NS1 proteins, of currently circulating H3N2 strains do not inhibit the activation of IRF3 and IFN-β transcription, whereas the NS1 proteins of currently circulating H1N1 strains do inhibit these activations (Kuo, Zhao et al. 2010). The NS1 proteins of H5N1 viruses were also found to inhibit these activations.

In a second mechanism, the NS1 protein of human influenza A viruses binds the 30kDa-subunit of the cleavage and polyadenylation specificity factor (CPSF30), a protein required for the 3′ end processing of cellular pre-mRNAs, thereby inhibiting production of IFN-β mRNA. The NS1 proteins of pathogenic 1997 H5N1 viruses contain the CPSF30-binding site but lack the consensus amino acids at position 103 and 106, F and

M, respectively that are required for the stabilization of CPSF30 binding. Instead they have L at position 103 and I at position 106. This results in non-optimal CPSF30 binding in infected cells and attenuated replication in tissue culture cells (Das, Ma et al. 2008; Kuo and Krug, 2009; Twu, Kuo et al. 2007). Thus, changing L103 to F and I106 to M in the HK97 NS1 protein results in a 20-fold increase in the rate of virus replication in MDCK cells, coupled with a 9-fold decrease in the production of IFN-β mRNA, indicating that the wild-type (wt) HK97 virus is impaired in its ability to suppress IFN-β and presumably other antiviral effectors in the host cell. Consequently, even though the H5N1 NS1 protein apparently inhibits the activation of IRF3 and IFN-β transcription, strong CPSF30 binding to the NS1 protein is still required for optimum replication and suppression of the IFN response.

Variations in NS1 proteins function have previously been linked to altered influenza virus virulence in laboratory animals (Imai, Shinya et al. 2010; Jang, Boltz et al. 2009). Because over 98% of highly pathogenic H5N1 viruses analyzed since 2003 possess the consensus amino acids F103 and M106 in the NS1 protein, we sought to understand the role of this motif, and therefore of high-affinity CPSF30 binding, in the virulence of H5N1 viruses. Here, we have demonstrated that strengthening CPSF30 binding, by changing positions 103 and 106 in the 1997 H5N1 NS1 protein to the consensus amino acids, results in a remarkable 300-fold increase in the lethality of the virus in mice. Unexpectedly, this increase in virulence is not associated with increased lung pathology but rather is characterized by faster systemic spread of the virus, particularly to the brain, where increased replication and severe pathology occur. This

increased spread is associated with increased cytokine and chemokine levels in extrapulmonary tissues determined by microarrays. Therefore, strengthening CPSF30 binding by the NS1 protein of 1997 H5N1 viruses enhances virulence in mice by increasing the systemic spread of the virus from the lungs, particularly to the brain.

3.2 MATERIALS AND METHODS

We hypothesized that changing amino acids in the NS1 protein from L and I at position 103 and 106 in the wild type A/Hong Kong/483/1997 (wtHK97) virus to F and M respectively, should result in increased virulence in mice. In order to test this we conducted experiments in collaboration with Dr. Ruben Donis at the Centers for Disease control and prevention (CDC).

Generation of mutant viruses by reverse genetics

Wild type (wt) A/Hong Kong/483/1997 (HK97) (subtype H5N1) and the HK97G2+ mutant were generated using a plasmid-based reverse genetics system. To generate the HK97G2+ virus, codons 103 and 106 of the NS1 open reading frame were changed from L (TTA) and I (ATT) to F (TTC) and M (ATG) respectively using standard oligonucleotide mutagenesis methods. Plasmid DNA was transfected into co-cultured 293T/MDCK cells and recombinant viruses were amplified and titered by plaque assay on MDCK cells as described previously. The eight genomic RNA segments of the recombinant viruses were sequenced to confirm the presence of the appropriate wild-type or mutant base at each position. All experiments with the recombinant HK97 viruses were performed in compliance with the Institutional Biosafety committee and NIH

guidelines for research involving recombinant DNA molecules. Viruses were handled in a biosafety level 3 laboratory at CDC, including enhancement required by the U.S department of agriculture and the select agents program (http://www/cdc.gov/od/ohs/biosfty/bmbl5/bmbl5toc.htm)

Mice

Eight-to-nine-week-old female BALB/c mice (Jackson Laboratories, Bar Harbor, ME) were used in this study. Mice were anesthetized by isoflurane inhalation and inoculated intranasally with 50µl of virus diluted in phosphate-buffered saline (PBS), pH 7.4, for uninfected controls. All animal studies were conducted according to protocols approved by the CDC institutional animal care and use committee. Groups of 5 animals were inoculated with 0.01 to 1000 PFU of virus in 10 fold-infectious dose increments. Mice in each group were weighed and monitored daily for survival and clinical signs for 14 days after infection. Animals with neurological signs or with severe weight loss (> or = to 25%) were euthanized, and the event was considered a lethal endpoint. Fifty percent mouse lethal dose (MLD_{50}) was calculated using cumulative survival data and expressed in PFU.

Virus replication *in vivo*

To study the kinetics of virus replication *in vivo,* mice were intranasally inoculated with wt HK97 or HK97G2+ virus. Lungs, spleen and brain were collected after infection, frozen on dry ice and stored at -80 ^{0} C until further processing. Organs were thawed, homogenized in 1ml of cold PBS, pH 7.4, using a Magnalyzer system and polystyrene beads and clarified by centrifugation (2,200 g) at 4^0C. Virus titers were

determined by plaque assay in MDCK cells; the limit of detection of the assay was 5PFU/ml. Whole blood was collected after infection and coagulation was prevented with EDTA. The blood was fractionated into plasma, white blood cells and red blood cells by centrifugation over an 18.23 % Histodenz cushion at 225g. The 50% egg infectious dose (EID_{50}) was determined by inoculating groups of 6 eggs with 10 fold-dilutions of each fraction and testing for infection by hemagglutinin assay as previously described.

Histopathology

Lungs and brains from uninfected (n=4 per group) and infected (n=5 per group) animals were fixed in 10% formalin, and paraffin-embedded sections were stained with hemotoxylin and eosin. Immunohistochemistry for caspase-3 and terminal deoxynucleotidyltransferase-mediated dUTP-biotin nick end labeling (TUNEL) staining of lung sections were performed by Cureline Biopathology (San Francisco, CA).

Flow cytometry

Lung cells were collected and stained for flow cytometry. Mice were euthanized by isoflurane inhalation. To obtain leukocytes and other small infiltrated cells, lungs were perfused through the left ventricle with 3ml of PBS. Lungs were minced and incubated for 30 minutes.

Expression microarray analysis

Groups of 4 mice were infected with 100 PFU of wt HK97 or HK97G2+ virus by intranasal route. Animals were euthanized at 1, 2, 4 and 6 days after infection and brain, lung and spleen tissues were collected and immediately frozen at -80^0C. Total RNA was isolated using Trizol reagent and the PureLink, Micro-to-Midi total RNA purification

system (Invitrogen) according to the manufacturer's manual. The RNAs were pooled from the 4 mice for each virus and for each time point and were used for comparative microarray analysis. We used NimbleGen *Mus musculus* 12 plex microarrays; duplicate arrays were used for each RNA sample (for each virus, for each time point and for each organ). Ten micrograms of pooled total RNA was processed and labeled, following the standard NimbleGen protocol. RNA was converted into cDNA using the SuperScript II cDNA conversion kit (Invitrogen). Double-stranded cDNA was random-prime labeled with Cy3 nonamers and hybridized to the microarrays for 16 h at 42^0C. The arrays were washed, dried and scanned at 5μM resolution using GenePix 4000B microarray scanner (Molecular Devices, Sunnyvale, CA). Data were extracted from scanned images using the NimbleScan 2.2 version 5 software program (Roche NimbleGen). Briefly, TIFF images of the hybridized chips were analyzed, and the data were normalized using the quantile normalization and robust multiarray averaging (RMA) analysis tool in the NimbleScan 2.2 version 5 software package. The normalized data were then imported into the Arraystar software program for further analysis. The mean of the duplicate data was determined for each pair of arrays. The fold change in wt HK97 and HK97G2+ gene expression was then determined relative to that of the mock-infected animal (moderated *t* test). The data from the replicate arrays for each RNA sample showed minimal difference (r^2>0.95). Consequently the fold changes for individual mRNAs showed minimal difference between the two replicate arrays. Messenger RNAs from the data set that met the 2-fold change cutoff (P< or =0.05) were loaded into the DAVID webserver (http://david.abcc.ncifcrf.gov/) and search parameters were set to include all available

categories from the three gene ontologies (GOs): biological process, cellular component and molecular function. This program uses the Fisher exact test to determine significance.

3.3 RESULTS

3.3.1 HK97G2+ mutant virus is more virulent than the wt HK97 virus in the mouse model

We used reverse genetics to construct both wild-type A/Hong Kong/483/1997 (HK97) (subtype H5N1) (wt HK97) and a mutated version (HK97G2+) differing only in the NS1 protein, in which amino acids at positions 103 and 106 in wt HK97 virus were converted from L and I to the consensus amino acids F and M, respectively (Twu, Kuo et al. 2007). The relative virulences of these viruses were evaluated in mice infected intranasally. Following doses of 0.1 to 100 PFU, HK97G2+ -infected mice lost weight more quickly than wt-HK97-infected mice and most had to be euthanized 6 to 8 days after infection (Figure 3.1) The differences in virulence between wtHK97 and HK97G2+ was most obvious at a dose of 1.0 PFU. With the 1.0 PFU dose, all of the HK97G2+-infected mice had to be euthanized by day 8, whereas none of the wt-HK97-infected mice succumbed (Figure 3.1C). The median mouse lethal dose (MLD_{50}) was 300-fold lower for HK97G2+ than for wt HK97 (10 PFU for wt HK97 and 0.032 PFU for HK97G2+).

3.3.2 HK97G2+ rapidly disseminates systemically

We measured the titers of these two viruses in lung, peripheral blood, spleen and brain (Figure 3.2). After intranasal infection with 100 PFU of virus, both wt HK97 and

HK97G2+ replicated well in the respiratory tract. However, HK97G2+ reached somewhat higher levels in the lungs than did wt HK97 (ANOVA, P=0.01), particularly at early times after infection, when there was as much as a 5-fold difference (Figure 3.2 A). By 2 days after infection, HK97G2+ titers in the spleen were more than 10-fold higher than those of wt HK97 (Figure 3.2 C), indicating that HK97G2+ spreads systematically much more efficiently and earlier than wt HK97. Similarly, by day 2, HK97G2+ was detected in the brain while wt HK97 was not, and by 4 days postinfection, HK97G2+ titers in the brain were approximately 100-fold higher than those of wt HK97 (Figure 3.2 D). Regardless of the challenge dose, titers in brain at 4 days postinfection were higher for mice infected with HK97G2+ (Figure 3.2 E). Consequently, the total amount of HK97G2+ virus at days 2 and 4 in the lung, spleen and brain exceeds the total amount of the wt HK97 virus showing that the HK97G2+ virus replicated considerably more rapidly than the wt HK97 virus.

We also measured virus titers in plasma. HK97G2+ was readily detectable in plasma 24 hours postinfection at a much higher titer than that of wt HK97 (Figure 3.2 B), demonstrating increased viremia during HK97G2+ infection. These results indicate that enhancing the ability of wt HK97 NS1 to bind CPSF30 enables the HK97G2+ virus to rapidly and efficiently spread systemically through early, increased viremia, leading to more rapid and efficient infection of the spleen and brain.

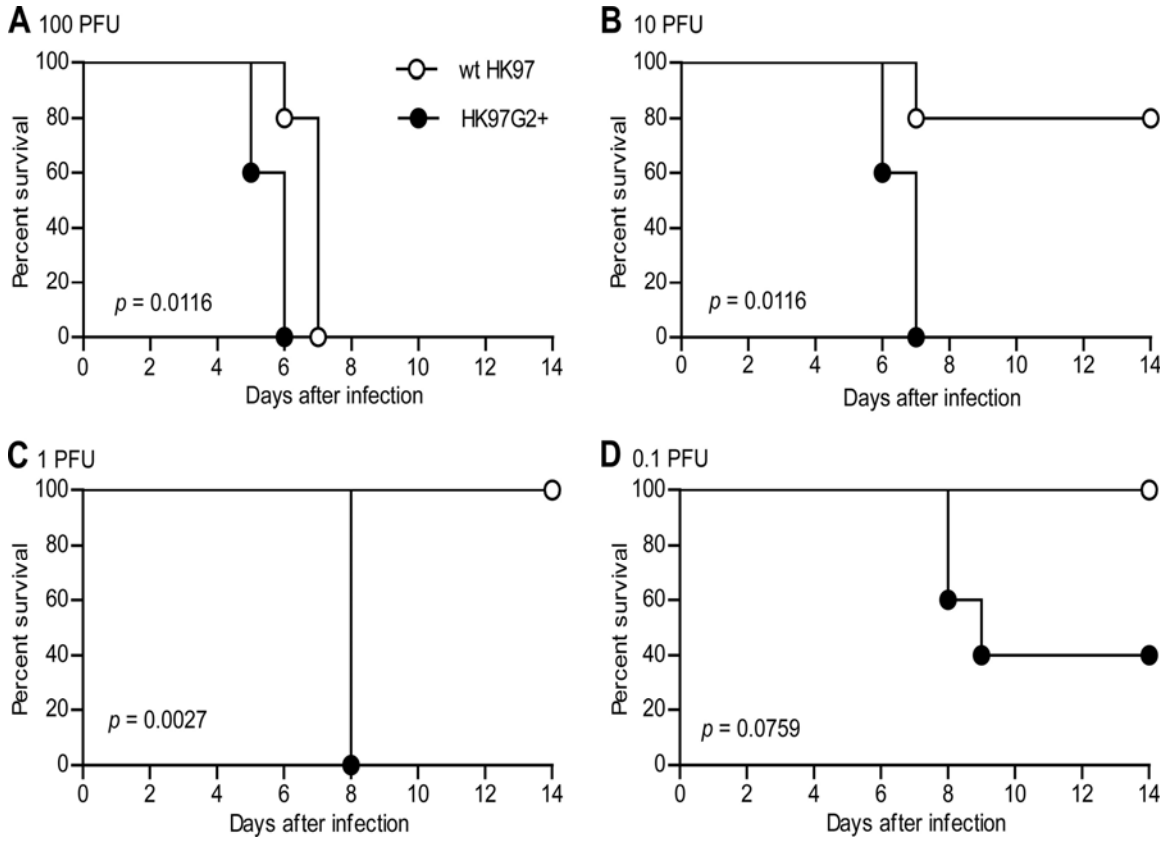

Figure 3.1 Survival of mice infected with wt HK97 or mutant HK97G2+ virus. BALB/c mice were infected in groups of 5 with 100 PFU (A), 10 PFU (B), 1 PFU (C), or 0.1 PFU (D) of indicated virus and monitored daily. Data represent 3 experiments with similar results

3.3.3 HK97G2+ spares the lungs but causes severe brain damage

Histopathological assessment of lungs from mice infected with 100 PFU of wt HK97 or HK97G2+ virus showed that infection with either virus led to moderate lung inflammation by 2 days postinfection, with some accumulation of neutrophils and exudates in the alveolar spaces. In mice infected with wt HK97, this damage progressed to bronchitis. In contrast, lung damage did not progress in HK97G2+. Similarly, analysis of apoptosis by caspase-3 staining indicated that while both viruses led to an increase in apoptotic and necrotic cells in the lungs, cell death was less marked in the airways of mice infected with HK97G2+.

We also assessed lung inflammation by using flow cytometry to analyze the number of innate and adaptive immune cells present in the lung. By 4 days after infection with wt HK97 virus, there was a >10 fold increases in the numbers of inflammatory monocytes, exudate macrophages and an almost 10 fold increase in the number of dendritic cells (Figure 3. 3 A to C). The increase in these cell types after HK97G2+ infection was significantly lower. Notably, by 6 days after infection, there were significantly fewer dendritic cells (Figure 3.2 B) and exudate macrophages (Figure 3.2 C) in the lungs of mice infected with HK97G2+. Other cell populations, particularly, B cells, CD4+ T cells and CD8+ T cells were less abundant in the lungs of HK97G2+-infected mice than in those of wt-HK97-infected mice (Figure 3.3 D to F). The overall smaller amounts of these innate and adaptive immune cells in the lungs of HK97G2+-infected

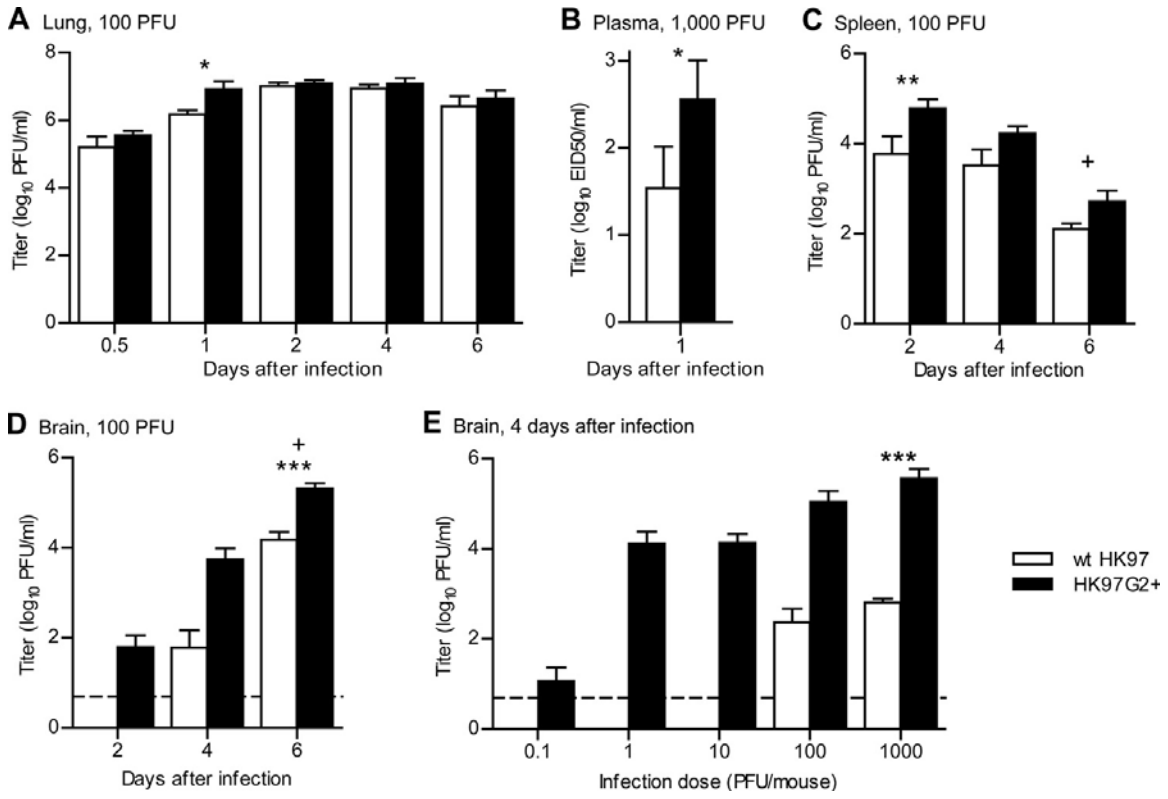

Figure 3.2 Replication kinetics of wt HK97 and HK97G2+ viruses in mice. BALB/c mice were infected intranasally with the indicated dose of virus. *****, p 0.05; ******* p 0.01; *******, p 0.001.For panels A (n = 4), C (n = 3) and D (n = 3), tissue was harvested at the indicated times and plaque assay was performed. For panel E (n = 3), mice were infected with the indicated PFU and tissue was harvested 4 days later for plaque assay. Data represent 3 experiments with similar results. The dotted line indicates the level of detection of the assay in cases where virus was not detected in one or more samples; for data below the detection level of the assay, the p value could not be determined. For panel B, blood from 5 mice was pooled 24 h after infection, plasma was separated, and the EID50 was determined. p values were calculated by Student's t test of the log-transformed values.

mice are further evidence of decreased lung inflammation after infection with the HK97G2+ virus.

Histopathological assessment of the brain showed substantially more brain pathology caused by the HK97G2+ virus than by the wt HK97 virus. In wt-HK97-infected mice, there was no evidence of changes to brain tissue until 4 days after infection, and most mice showed only mild changes with minimal cell death. In contrast, mild changes were already present in the brain by 2 days after infection with HK97G2+, which rapidly progressed to moderate cell death and meningitis in most mice by 6 days after infection. The extent of histopathological damage in the brain corresponded well to the amount of virus detected in the brain.

3.3.4 Spread of the HK97G2+ virus is associated with increased cytokine and chemokine levels in extrapulmonary tissues

We performed microarray analyses of cellular mRNAs in the lungs, spleen and brains of mice infected with the two viruses to determine whether cellular mRNAs encoding other cytokines and chemokines or for apoptotic proteins were upregulated during infection. Groups of four mice were infected with 100 PFU of either wt HK97 or HK97G2+ virus and tissues were collected at 1,2,4 and 6 days after infection. Another group of four mice was mock infected, and tissues were collected 2 days later. Total RNA was extracted, and the RNAs of each group of four mice were pooled and used for microarray analysis. We compared the mRNA profile of wt HK97-infected mice and HK97G2+-infected mice to the mRNA profile in the mock-infected mice as described in materials and methods. Messenger RNAs that increased by 2-fold or greater (P< or

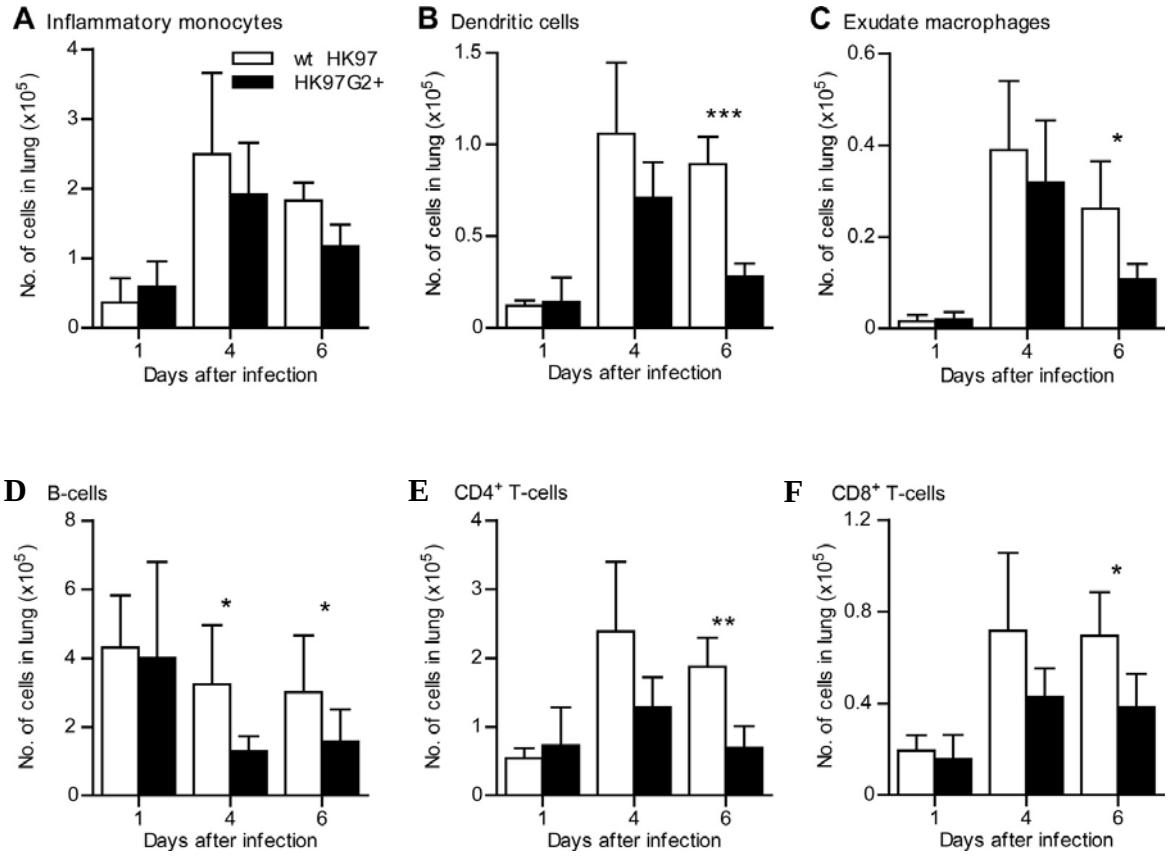

Figure 3.3 Inflammatory cells recruited to the lungs of mice after infection with wt HK97 and HK97G2+.

BALB/c mice in groups of 5 were infected with 100 PFU of virus, including a group of uninfected mice as a control. The absolute numbers of different immune cell subsets found in the lungs are shown. Bars indicate means with SD. *****, P 0.05; P 0.01; *******, P 0.001 by unpaired two-tailed Student's t test of results for wt HK97 compared to those for HK97G2+ at indicated times.

=0.05) in the tissues of the mice infected with either virus relative to levels for the mock-infected mice were categorized using the DAVID program (Dennis, Sherman et al. 2003)

Analysis of cellular gene expression in the lungs showed that the levels of many cytokine and chemokine mRNAs were substantially increased in mice infected with either wt HK97 or HK97G2+ virus at 1, 2,4 and 6 days postinfection relative to levels in mock-infected mice. This analysis detected increases in several (16-22) cytokine and chemokine mRNAs at 1 day postinfection. Of these, 5 were at higher levels in the HK97G2+ infected mice (CCL7, CXCL9, CCL12, IL-6 and TNF-α) and 4 were at higher levels in the wt HK97-infected mice (IL-23p19, IL-24,IL-4 and IL-31) (Table 3.1). At other days postinfection, there was no statistically significant difference in the levels of lung cytokine and chemokine mRNAs between the wt HK97 and HK97G2+-infected mice. In contrast, in the spleen the levels of cytokine and chemokine mRNAs at day 2 postinfection were significantly higher for the HK97G2+-infected mice. Representatives of such mRNAs are shown in Table 3.1. These mRNAs include a wide array of cytokines/chemokines (MCP-1, IFN-γ (lambda IFN [IFN-λ], CXCL11, CXC2, CXCL9, CCL4 and CCL12). The difference in the levels of these mRNAs between the two viruses decreased at later days postinfection. In addition, the microarray analysis revealed that increased levels of several mRNAs encoding apoptosis-related proteins were induced in the spleens of mice infected by either virus (Granzyme A[GzmA], Granzyme E[GzmE], Prf1, Granzyme C[GzmC] and Granzyme B [GzmB]).

Even more dramatic differences in the levels of cytokine and chemokine mRNAs between the two viruses occurred in the brain (Table 3.1). Thus, at 4 days postinfection,

Tissue and gene name	Fold increase in mRNA with infection							
	Day 1		Day 2		Day 4		Day 6	
	Wt HK97	HK97G2+	Wt HK97	HK97G2+	Wt HK97	HK97G2+	Wt HK97	HK97G2+
Lung								
CCL7	2.3	17.4	ND	ND	ND	ND	ND	ND
CXCL9	—	7.5	ND	ND	ND	ND	ND	ND
CCL12	—	5.4	ND	ND	ND	ND	ND	ND
IL-6	—	5.3	ND	ND	ND	ND	ND	ND
TNF-α	—	2.8	ND	ND	ND	ND	ND	ND
IL-23p19	4.1	—	ND	ND	ND	ND	ND	ND
IL-24	3.3	—	ND	ND	ND	ND	ND	ND
IL-4	2.9	—	ND	ND	ND	ND	ND	ND
IL-31	2.8	—	ND	ND	ND	ND	ND	ND
Spleen								
IFN-γ	ND	ND	9	28.2	22.8	30.6	3.4	3.6
CCL7	ND	ND	9.2	26.3	30.9	75.2	8.5	10.9
CXCL11	ND	ND	28.4	78.4	43.5	56	13	10.2
CXCL2	ND	ND	4.6	10.2	2.6	10.3	—	4.6
MCP-1	ND	ND	12.8	28.6	13.9	42.7	4.3	4.6
IFN-λ	ND	ND	8	17.3	6.8	2.3	—	—
IL-6	ND	ND	3.2	6.7	—	6.2	—	—
CXCL9	ND	ND	5.8	11.7	9.8	10.1	5.1	2.3
CCL4	ND	ND	7.5	14.6	3.6	12.5	—	3.2
CCL12	ND	ND	11.1	20.5	3.8	13.6	2.7	2.9
GzmA	ND	ND	—	2.5	3.2	4.5	2	2.4
GzmE	ND	ND	—	2.5	4.9	11	5	5.2
Prf1	ND	ND	—	2.2	2.3	3.4	—	—
GzmC	ND	ND	2.9	4.7	4.1	25.4	8.8	16.7
GzmB	ND	ND	15.6	21.8	16.3	32	14.8	19.5
Brain								
CCL12	ND	ND	—	2	—	10.6	10.7	20.1
ISG15	ND	ND	2	4.5	2.7	12.1	9.1	41.4
DDX58	ND	ND	—	2.1	—	4.4	4.3	16.8
IFI16	ND	ND	—	—	—	4.4	6.6	29.3
CXCL11	ND	ND	—	2.5	2.9	10.7	6.7	46
IFIH1	ND	ND	—	—	—	3.1	4.1	17.3
MxA	ND	ND	—	2.1	2.1	6.3	6.8	31.9
CCL7	ND	ND	—	—	—	2.7	4.5	24.8
IRF7	ND	ND	2.8	6.5	4.7	12.5	11.5	46.4
OAS1	ND	ND	—	2.1	2	4.7	4.3	19.5
MCP-1	ND	ND	—	—	—	2.3	4.2	49.5
IFIT2	ND	ND	—	2.8	2.3	5.7	8.5	38.5
IFIT3	ND	ND	2.7	4.2	3.4	7.6	7.9	18.1
IFITM3	ND	ND	—	2.1	2.7	5.1	4.8	11.7
IRF1	ND	ND	—	2.1	2.3	4.1	8	45.4
CXCL10	ND	ND	12.3	15.3	7.8	11.5	6.9	58.1

Table 3.1 Activation of cytokine and chemokine mRNAs in various organs of wt HK97 and HK97G2+ virus-infected mice.

Chemokine and cytokine mRNAs that were increased by at least 2-fold in the organs of infected mice relative to levels for mock-treated mice are shown. "_" indicates that these transcripts did not meet the 2-fold-change cutoff at these times after infection. ND, no data.

the levels of a large group of these mRNAs in the brain were substantially higher in HK97G2+ -infected mice than in wt-HK97-infected mice. By 6 days postinfection the difference in the levels of these mRNAs increased further, ranging from a 3-to 10-fold difference. Again, these results are consistent with the much earlier and more extensive infection of the brain with the HK97G2+ virus and with the increased brain pathology caused by the HK97G2+ virus.

We measured a subset of cytokines and chemokines in lung, spleen and brain after infection of mice with 100PFU of wtHK97 or HK97G2+ at 2 and 4 days postinfection, using ELISA and cytometric bead array assays. In the lung both viruses induced similar levels of type I and type II IFNs and cytokines which was consistent with the microarray analyses. Furthermore, the levels of cytokines and chemokines in the spleen and brain were much higher in the HK97G2+-infected mice than in wt-HK97-infected mice which correlated well with our microarray analyses (data not shown).

3.4 DISCUSSION

Pathogenic 1997 H5N1 viruses are lethal for chickens and humans in nature and in laboratory experiments they are lethal for mice and ferrets (Claas, Osterhaus et al. 1998; Gambotto, Barratt-Boyes et al. 2008; Hatta, Gao et al. 2001). These H5N1 viruses were highly virulent despite the fact that their encoded NS1 proteins contain a defect in one of their major functions directed at countering the host antiviral (IFN) response, namely, the binding of CPSF30 which causes the suppression of the production of mature cytoplasmic cellular mRNAs including IFN-β mRNA and presumably other antiviral

mRNAs (Das, Ma et al. 2008; Kim, Latham et al. 2002; Kuo, Zhao et al. 2010). Strong binding of CPSF30 requires the presence of F and M at positions 103 and 106, respectively, in the NS1 protein (Twu, Kuo et al. 2007). Instead of these two amino acids, the NS1 proteins of pathogenic 1997 H5N1 viruses contain L and I respectively, at positions 103 and 106 and as a consequence bind CPSF30 non-optimally. Changing these two amino acids in the HK97 NS1 protein to the post-2003 consensus residues in the NS1 proteins of H5N1 viruses (F and M at 103 and 106, respectively) strengthens CPSF30 binding and enhances virus replication in tissue culture (Twu, Kuo et al. 2007). In the present study, we demonstrated that changing these two NS1 amino acids to the consensus amino acids leads to a very dramatic (300-fold) increase in the lethality of the virus in mice.

Our results indicate that this enhanced virulence of HK97G2+ is likely due to its earlier and more efficient replication and systemic spread. After intranasal inoculation with HK97G2+ but not wt HK97, virus was readily detected in blood within 24 hours of infection. Consistent with this rapid establishment of viremia, HK97G2+ also reached much higher titers in the spleen by 2 days and in the brain by 4 days. The total amount of HK97G2+ virus at days 2 and 4 in the lung, spleen and brain substantially exceeds the total amount of the wt HK97 virus showing that the HK97G2+ virus replicated considerably more rapidly than the wt HK97 virus. However, the titer of the HK97G2+ virus in the lung was only slightly higher than that of the wt HK97 virus. It is likely that this relatively smaller difference in titers reflects the fact that the HK97G2+ virus not only replicates more rapidly in the lungs but also spreads more rapidly from the lungs.

Such a rapid dissemination from the lung would explain why the HK97G2+ virus caused less damage and cell death in the lungs and attracted fewer infiltrating inflammatory cells into the lungs than did the wt HK97 virus. In addition, the host cytokine response in the lung was essentially the same as the cytokine response in the lung to wt HK97 virus infection from 2 to 6 days post infection.

In contrast, the cytokine and chemokine levels in the spleen and brain, as measured by both direct protein assays and microarray analysis, were much higher in HK97G2+-infected mice than in wt HK97-infected mice. These differences largely mirrored the time course of accumulation of the two viruses in these two organs. On day 2 postinfection, the HK97G2+ virus achieved a considerably higher titer than the wt HK97 virus in the spleen and the HK97G2+ virus induced higher chemokine and cytokine mRNA levels in the spleen on this day. Similarly, the HK97G2+ virus spread to the brain faster than the wtHK97 virus, where it replicated faster, and the chemokine and cytokine mRNA levels in the brain at 4 and 6 days postinfection were much larger after HK97G2+ virus infection. We interpret these results to indicate that the increased levels of the cytokines and chemokines produced in the spleen and brain after HK97G2+ virus infection represent mostly the responses of local uninfected cells, including trafficking immune cells, to increased viral loads in these two organs.

Consistent with the more rapid spread and replication of the HK97G2+ virus in the brain, mice infected with HK97G2+ but not with wt HK97 exhibited extensive brain damage by 6 days post infection, at which point most mice infected with HK97G2+ succumbed to infection. Our results fit a model in which the lung is site of initial

enhanced replication by the HK97G2+ virus, but lethality results from rapid dissemination to other organs, particularly to the brain, where severe pathology occurred. Spread of wt HK97 virus to the brain was also observed in previous studies (Tanaka, Park et al. 2003). However, a recent study has provided evidence that the wt HK97 virus kills mice by rapid replication in the lungs that overcomes the host immune response (Hatta, Hershberger et al. 2010).

In contrast to the H5N1 HK97 NS1 protein, CPSF30 binding by the NS1 protein of H1N1 viruses appears to be less critical for optimal suppression of the host antiviral response. For example, the NS1 protein of the 2009 H1N1 virus does not bind CPSF30, because the consensus binding site is blocked by other NS1 amino acids. Removal of this block leading to the establishment of CPSF30 binding has only a minimal effect on IFN production, virus replication and mouse virulence (Hale, Steel et al. 2010). An important issue is therefore why strong CPSF30 binding by the NS1 protein of the H5N1 HK97 virus is required for optimal suppression of the host antiviral response. One possibility is that the suppression of the activation of IRF3 and IFN-β transcription by the NS1 protein of H5N1 viruses is actually not as effective as the suppression mediated by the NS1 protein of H1N1 viruses and that his difference has not yet been detected by the methods that have so far been employed. It has already been established that the NS1 proteins of different influenza A virus subtypes differ in their ability to suppress the activation of IRF3 and IFN-β transcription. The NS1 proteins of human H2N2 and H3N2 strains do not inhibit the activation of IRF3 and IFN-β transcription, whereas the NS1 proteins of currently circulating H1N1 strains do inhibit these activations (Kuo, Zhao et al. 2010).

Perhaps the NS1 proteins of H1N1 and H5N1 viruses also differ, specifically in the extent to which they inhibit the activation of IRF3 and IFN-β transcription.

It will be important to elucidate the mechanism by which the HK97G2+ virus rapidly disseminates from the lung and enters the brain. For some H5N1 viruses, neurotropic spread via the vagus nerve to the brain has been demonstrated (Jang, Boltz et al. 2009; Tanaka, Park et al. 2003). In the present case, an alternate possibility is suggested by our finding that the HK97G2+ virus but not the wt HK97 virus was readily detected in blood within 24 hours of infection, indicating that HK97G2+ might increase pulmonary vascular permeability, thereby establishing viremia at very early times of infection. At day 1 postinfection, MCP-1 and TNF-α were increased in HK97G2+-infected lungs compared to levels in wt HK97-infected lungs. These two cytokines are known to increase pulmonary vascular permeability (Lee, Liu et al. 2006; Mazzon and Cuzzocrea, 2007) which has previously been implicated in influenza virus pathogenesis (Wang, Zhao et al. 2010). This early viremia would enable HK97G2+ to rapidly seed peripheral organs such as the spleen and subsequently spread to the brain, where cytokinemia may also increase the permeability of the blood-brain barrier, whereas the wild-type virus may be restricted to slower neurotropic spread through peripheral nerves.

Our results with the HK97G2+ virus, coupled with a recent study of the wt HK97 virus (Tanaka, Park et al. 2003), indicate that a two amino-acid change in the NS1 protein likely leads to a dramatic change in the site of severe pathology induced by the HK97 virus, from the lung to the brain. The results fit a model in which the lung is the site of initial enhanced replication by the HK97G2+ virus but lethality results from rapid

dissemination to other organs, particularly the brain, where severe pathology occurred. Therefore, changing the NS1 amino acids at positions 103 and 106 to F and M, respectively, enables the 1997 H5N1 virus to replicate more rapidly and to spread throughout the body more efficiently, particularly to the brain, dramatically increasing its virulence.

REFERENCES

Akkina, R. K., Chambers, T. M et al. (1987)." Intracellular localization of the viral polymerase proteins in cells infected with influenza virus and cells expressing PB1 protein from cloned cDNA." *Journal of virology*, *61*(7), 2217-24.

Arimoto, K., Takahashi, H et al. (2007)." Negative regulation of the RIG-I signaling by the ubiquitin ligase RNF125." *Proceedings of the National Academy of Sciences of the United States of America*, *104*(18), 7500-5.

Boulo, S., Akarsu, H et al. (2007)." Nuclear traffic of influenza virus proteins and ribonucleoprotein complexes." *Virus research*, *124*(1-2), 12-21.

Boyle, K. A., Pietropaolo, R. L et al. (1999). "Engagement of the cellular receptor for glycoprotein B of human cytomegalovirus activates the interferon-responsive pathway." *Molecular and cellular biology*, *19*(5), 3607-13.

Carr, C. M. and Kim C. S. (1994). "Flu virus invasion: halfway there." *Science*, *266*(5183), 234-6.

Chen, H., Bright, R. A et al. (2007). "Polygenic virulence factors involved in pathogenesis of 1997 Hong Kong H5N1 influenza viruses in mice." *Virus research*, *128*(1-2), 159-63.

Chien, C.-ya, Xu, Y et al. (2004). "Biophysical characterization of the complex between double-stranded RNA and the N-terminal domain of the NS1 protein from influenza A virus: evidence for a novel RNA-binding mode." *Biochemistry*, *43*(7), 1950-62.

Civril, F., Bennett, M et al. (2011)." The RIG-I ATPase domain structure reveals insights into ATP-dependent antiviral signalling. "*EMBO reports*, *12*(11), 1128-1135.

Claas, E. C., Osterhaus, A. D et al. (1998). "Human influenza A H5N1 virus related to a highly pathogenic avian influenza virus." *Lancet*, *351*(9101), 472-7.

Cui, Y., Li, M et al. (2001). "The Stat3/5 locus encodes novel endoplasmic reticulum and helicase-like proteins that are preferentially expressed in normal and neoplastic mammary tissue." *Genomics*, *78*(3), 129-34.

Das, K., Ma, L.-C et al. (2008). "Structural basis for suppression of a host antiviral response by influenza A virus." *Proceedings of the National Academy of Sciences of the United States of America*, *105*(35), 13093-8.

Dennis, G., Sherman, B. T et al. "DAVID: Database for Annotation, Visualization, and Integrated Discovery." *Genome biology*, *4*(5), P3.

Diao, F., Li, Shu et al. (2007). "Negative regulation of MDA5- but not RIG-I-mediated innate antiviral signaling by the dihydroxyacetone kinase." *Proceedings of the National Academy of Sciences of the United States of America*, *104*(28), 11706-11.

Dias, A., Bouvier, D et al. (2009). "The cap-snatching endonuclease of influenza virus polymerase resides in the PA subunit." *Nature*, *458*(7240), 914-8.

Du, W (1992). "An ATF/CREB Binding Site Protein is Required for Virus Induction of the Human Interferon Gene." *Proceedings of the National Academy of Sciences*, *89*(6), 2150-2154.

Egorov, A., Brandt, S et al.(1998). "Transfectant influenza A viruses with long deletions in the NS1 protein grow efficiently in Vero cells." *Journal of virology*, *72*(8), 6437-41.

Ehrhardt, C., and Ludwig, S. (2009)." A new player in a deadly game: influenza viruses and the PI3K/Akt signalling pathway." *Cellular microbiology*, *11*(6), 863-71.

Fujita, T., Miyamoto, M et al. (1989). "Involvement of a cis-element that binds an H2TF-1/NFkB like factor(s) in the virus-induced interferon-beta gene expression". *Nucleic Acids Research*, *17*(9), 3335-3346.

Fujita, T., Onoguchi, K et al. (2007)." Triggering antiviral response by RIG-I-related RNA helicases." *Biochimie*, *89*(6-7), 754-60.

Gack, M. U., Shin, Y. C et al. (2007). "TRIM25 RING-finger E3 ubiquitin ligase is essential for RIG-I-mediated antiviral activity." *Nature*, *446*(7138), 916-920.

Gambotto, A., Barratt-Boyes S. M et al. (2008). "Human infection with highly pathogenic H5N1 influenza virus." *Lancet*, *371*(9622), 1464-75.

Garaigorta, U. (2007)." Mutation analysis of a recombinant NS replicon shows that influenza virus NS1 protein blocks the splicing and nucleo-cytoplasmic transport of its own viral mRNA." *Nucleic acids research*, *35*(14), 4573-4582.

Garcia-Sastre A, Egorov. A et al (1998). "Influenza A virus lacking the NS1 gene replicates in interferon-deficient systems." *Virology*, *252*(2), 324-330.

Goodbourn, S., Didcock, L et al. (2000). "Interferons : cell signalling , immune modulation , antiviral responses and virus countermeasures." *Journal of General Virology*, 2341-2364.

Gorbalenya, A. E. and Koonin. E. V. (1988)." One more conserved sequence motif in helicases." *Nucleic acids research*, *16*(15), 7734.

Greenspan, D., Palese, P et al. (1988)." Two nuclear location signals in the influenza virus NS1 nonstructural protein." *Journal of virology*, *62*(8), 3020-6.

Guan, Y., Poon, L. L. M et al. (2004). "H5N1 influenza: a protean pandemic threat." *Proceedings of the National Academy of Sciences of the United States of America*, *101*(21), 8156-61.

Hale, B. G., Steel, J et al. (2010). "Inefficient control of host gene expression by the 2009 pandemic H1N1 influenza A virus NS1 protein." *Journal of virology*, *84*(14), 6909-22.

Haller, O., Kochs, G et al.(2006). "The interferon response circuit: induction and suppression by pathogenic viruses." *Virology*, *344*(1), 119-30.

Hatta, M., Gao, P et al. (2001). "Molecular basis for high virulence of Hong Kong H5N1 influenza A viruses." *Science*, *293*(5536), 1840-2.

Hatta, Y., Hershberger, K et al. (2010). "Viral replication rate regulates clinical outcome and CD8 T cell responses during highly pathogenic H5N1 influenza virus infection in mice." *PLoS pathogens*, *6*(10) e1001139.

Hernandez, L. D., Hoffman, L. R et al. (1996). "Virus-cell and cell-cell fusion." *Annual review of cell and developmental biology*, *12*, 627-61.

Hiscott, J. (2007). "Triggering the innate antiviral response through IRF-3 activation." *The Journal of biological chemistry*, *282*(21), 15325-9.

Honda A., Ueda K et al. (1988). "The role of interferon in influenza virus tissue tropism." *J Biochem*, *104*(6), 1021-6.

Horimoto, T. and Kawaoka, Y. (1994). "Reverse genetics provides direct evidence for a correlation of hemagglutinin cleavability and virulence of an avian influenza A virus." *Journal of virology*, *68*(5), 3120-8.

Hornung, V., Ellegast, J et al. (2006). "5'-Triphosphate RNA is the ligand for RIG-I." *Science*, *314*(5801), 994-7.

Imai, H., Shinya, K et al. (2010). "The HA and NS genes of human H5N1 influenza A virus contribute to high virulence in ferrets." *PLoS pathogens*, *6*(9) e1001106.

Ito, T. (2000)." Interspecies transmission and receptor recognition of influenza A viruses." *Microbiology Immunolog 44*(6), 423-30.

Jang, H., Boltz, D et al. (2009). "Highly pathogenic H5N1 influenza virus can enter the central nervous system and induce neuroinflammation and neurodegeneration." *Proceedings of the National Academy of Sciences of the United States of America*, *106*(33), 14063-8.

Jiang, F., Ramanathan, A et al.(2011). "Structural basis of RNA recognition and activation by innate immune receptor RIG-I." *Nature*, 1-7.

Jing, X., Ma, C et al.(2008)." Functional studies indicate amantadine binds to the pore of the influenza A virus M2 proton-selective ion channel." *Proceedings of the National Academy of Sciences of the United States of America*, *105*(31), 10967-72.

Jones, I. M., Reay, P. A et al.(1986). "Nuclear location of all three influenza polymerase proteins and a nuclear signal in polymerase PB2." *The EMBO journal*, *5*(9), 2371-6.

Kageyama, M., Takahashi, K et al.(2011). "55 amino acids linker between helicase and carboxyl terminal dmoains of RIG-I functions as a critical repression domain and determines inter-domain conformation." *Biochem Biophys Res Commun 415,* 75-81.

Kandun, I. N., Tresnaningsih, E et al.(2008). "Factors associated with case fatality of human H5N1 virus infections in Indonesia: a case series." *Lancet*, *372*(9640), 744-9.

Kato, H., Takeuchi, O et al. (2006). "Differential roles of MDA5 and RIG-I helicases in the recognition of RNA viruses." *Nature*, *441*(7089), 101-5.

Kim, M.-J., Latham, A. G et al.(2002)." Human influenza viruses activate an interferon-independent transcription of cellular antiviral genes: outcome with influenza A virus is unique." *Proceedings of the National Academy of Sciences of the United States of America*, *99*(15), 10096-101.

Kochs, G., García-Sastre, A et al.(2007). "Multiple anti-interferon actions of the influenza A virus NS1 protein." *Journal of virology*, *81*(13), 7011-21.

Komuro, A. and Horvath, C. M. (2006). "RNA- and virus-independent inhibition of antiviral signaling by RNA helicase LGP2." *Journal of virology*, *80*(24), 12332-42.

Kowalinski, E., Lunardi, T et al.(2011)." Structural Basis for the Activation of Innate Immune Pattern-Recognition Receptor RIG-I by Viral RNA." *Cell*, *147*(2), 423-35.

Krug, R. M. and Etkind P. R. (1973)." Cytoplasmic and Nuclear virus-specific proteins in Influenza virus-infected MDCK cells." *Virology*, *56*(56), 334-348.

Krug, R., Yuan, W et al. (2003). "Intracellular warfare between human influenza viruses and human cells: the roles of the viral NS1 protein." *Virology*, *309*(2), 181-189.

Kuo, R.-L. and Krug, R. M. (2009)." Influenza a virus polymerase is an integral component of the CPSF30-NS1A protein complex in infected cells." *Journal of virology*, *83*(4), 1611-6.

Kuo, R.-L., Zhao, C et al. (2010). "Influenza A virus strains that circulate in humans differ in the ability of their NS1 proteins to block the activation of IRF3 and interferon-β transcription." *Virology*, *408*(2), 146-58.

Lamb, R. A. and Lai, C. J. (1980). "Sequence of interrupted and uninterrupted mRNAs and cloned DNA coding for the two overlapping nonstructural proteins of influenza virus." *Cell*, *21*(2), 475-485.

Lamb, R. A. and Krug, R.M. (2001). *Orthomyxoviridae: the viruses and their replication. In Fields Virology, (D. M. Knipe and P.M. Howley, eds.)* (pp. 1487-1531).

Lazarowitz, S G., Compans, R. W et al. (1971). "Influenza Virus Structural Ceils and and Their Nonstructural Plasma Proteins in Infected Membranes ".*Virology*,*46,*830-843.

Lee, Y.-R., Liu, M.-T et al. (2006). "MCP-1, a highly expressed chemokine in dengue haemorrhagic fever/dengue shock syndrome patients, may cause permeability change, possibly through reduced tight junctions of vascular endothelium cells." *The Journal of general virology*, *87*(12), 3623-30.

Li, M. L., Rao, P et al. (2001). "The active sites of the influenza cap-dependent endonuclease are on different polymerase subunits." *The EMBO journal*, *20*(8), 2078-86.

Li, X., Ranjith-Kumar, C. T et al.(2009)." The RIG-I-like receptor LGP2 recognizes the termini of double-stranded RNA." *The Journal of biological chemistry*, *284*(20), 13881-91.

Luo, D., Ding, S. C et al.(2011)."Structural Insights into RNA Recognition by RIG-I." *Cell*, *147*(2), 409-22.

Mazzon, E. and Cuzzocrea, S. (2007). "Role of TNF-alpha in lung tight junction alteration in mouse model of acute lung inflammation." *Respiratory research*, *8*, 75.

McAuley, J. L., Zhang, K et al.(2010). "The effects of influenza A virus PB1-F2 protein on polymerase activity are strain specific and do not impact pathogenesis." *Journal of virology*, *84*(1), 558-64.

Medcalf, L., Poole, E et al. (1999). "Temperature-Sensitive Lesions in Two Influenza A Viruses Defective for Replicative Transcription Disrupt RNA Binding by the Nucleoprotein Temperature-Sensitive Lesions in Two Influenza A Viruses Defective for Replicative Transcription Disrupt RNA Binding." *Journal of Virology, 73*(9), 7349-56.

Melén, K., Kinnunen, L et al.(2007). "Nuclear and nucleolar targeting of influenza A virus NS1 protein: striking differences between different virus subtypes." *Journal of virology*, *81*(11), 5995-6006.

Meylan, E., Curran, J et al.(2005)." Cardif is an adaptor protein in the RIG-I antiviral pathway and is targeted by hepatitis C virus." *Nature*, *437*(7062), 1167-72.

Mibayashi, M., Martínez-Sobrido, L et al.(2007). "Inhibition of retinoic acid-inducible gene I-mediated induction of beta interferon by the NS1 protein of influenza A virus." *Journal of virology*, *81*(2), 514-24.

Min, J.-Y and Krug, R. M. (2006). "The primary function of RNA binding by the influenza A virus NS1 protein in infected cells: Inhibiting the 2'-5' oligo (A) synthetase/RNase L pathway." *Proceedings of the National Academy of Sciences of the United States of America*, *103*(18), 7100-5.

Min, J.-Y., Li, S et al. (2007). "A site on the influenza A virus NS1 protein mediates both inhibition of PKR activation and temporal regulation of viral RNA synthesis." *Virology*, *363*(1), 236-43.

Miyoshi, K., Cui, Y et al.(2001). "Structure of the mouse Stat 3/5 locus: evolution from Drosophila to zebrafish to mouse." *Genomics*, *71*(2), 150-5.

Murali, A., Li, X et al.(2008). "Structure and function of LGP2, a DEX(D/H) helicase that regulates the innate immunity response." *The Journal of biological chemistry*, *283*(23), 15825-33.

Naffakh, N., Tomoiu, A et al. (2008). "Host restriction of avian influenza viruses at the level of the ribonucleoproteins." *Annual review of microbiology*, *62*, 403-24.

Navarro, L., Mowen, K et al. (1998). "Cytomegalovirus Activates Interferon Immediate-Early Response Gene Expression and an Interferon Regulatory Factor 3-Containing Interferon-Stimulated Response Element-Binding Complex Cytomegalovirus Activates Interferon Immediate-Early Response Gene Expression." *Molecular and Cellular Biology*, *18*(7), 3796.

Neill, R. E. O and Jaskunas, R. (1995). "Nuclear Import of Influenza Virus RNA Can Be Mediated by Viral Nucleoprotein and for Protein Import ." *Biochemistry*, *270,*(39) 22701-22704.

Nemeroff, M. E., Barabino, S. M et al. (1998)." Influenza virus NS1 protein interacts with the cellular 30 kDa subunit of CPSF and inhibits 3'end formation of cellular pre-mRNAs." *Molecular cell*, *1*(7), 991-1000.

Neumann, G., Hughes, M. T et al (2000). "Influenza A virus NS2 protein mediates vRNP nuclear export through NES-independent interaction with hCRM1." *The EMBO journal*, *19*(24), 6751-8.

Newby, C. M., Sabin, L et al.(2007). "The RNA binding domain of influenza A virus NS1 protein affects secretion of tumor necrosis factor alpha, interleukin-6, and interferon in primary murine tracheal epithelial cells." *Journal of virology*, *81*(17), 9469-80.

Newcomb, L. L., Kuo, R.-L et al. (2009). "Interaction of the influenza a virus nucleocapsid protein with the viral RNA polymerase potentiates unprimed viral RNA replication." *Journal of virology*, *83*(1), 29-36.

Nieto, A., de la Luna, S et al.(1994)." Complex structure of the nuclear translocation signal of influenza virus polymerase PA subunit." *The Journal of general virology*, *75* (1), 29-36.

Noah, D., Twu K. Y et al. (2003)." Cellular antiviral responses against influenza A virus are countered at the posttranscriptional level by the viral NS1A protein via its binding to a cellular protein required for the 3′ end processing of cellular pre-mRNAS." *Virology*, *307*(2), 386-395.

Osterhaus, A. D. (2000)." Influenza B Virus in Seals." *Science*, *288*(5468), 1051-1053.

O'Neill, L. A. J and Bowie, A. G. (2011). "The Powerstroke and Camshaft of the RIG-I Antiviral RNA Detection Machine." *Cell*, *147*(2), 259-61.

O'Neill, R. E., Talon, J et al.(1998). "The influenza virus NEP (NS2 protein) mediates the nuclear export of viral ribonucleoproteins." *The EMBO journal*, *17*(1), 288-96.

Peiris, J. S. M., Yu, W. C et al. (2004). "Re-emergence of fatal human influenza A subtype H5N1 disease." *Lancet*, *363*(9409), 617-9.

Pichlmair, A., Schulz, O et al.(2006)." RIG-I-mediated antiviral responses to single-stranded RNA bearing 5'-phosphates." *Science*, *314*(5801), 997-1001.

Pichlmair, A., Schulz, O et al.(2009). "Activation of MDA5 requires higher-order RNA structures generated during virus infection." *Journal of virology*, *83*(20), 10761-9.

Pinto, L. H. and Lamb, R. A (2006). "The M2 proton channels of influenza A and B viruses." *The Journal of biological chemistry*, *281*(14), 8997-9000.

Pinto, L. H., Holsinger. L. J et al. (1992). "Influenza Virus M2 portein Has Ion Channel Activity." *Cell*, *69*, 517-528.

Pippig, D. A., Hellmuth, J. C et al.(2009). "The regulatory domain of the RIG-I family ATPase LGP2 senses double-stranded RNA." *Nucleic acids research*, *37*(6), 2014-25.

Plotch, S. J., Bouloy, M et al.(1981)." A unique cap(m7GpppXm)-dependent influenza virion endonuclease cleaves capped RNAs to generate the primers that initiate viral RNA transcription. "*Cell*, *23*(3), 847-58.

Pollpeter, D., Komuro, A et al. (2011). "Impaired cellular responses to cytosolic DNA or infection with Listeria monocytogenes and vaccinia virus in the absence of the murine LGP2 protein." *PloS one*, *6*(4), e18842.

Poon, L. L., Pritlove, D. C et al. (1999)." Direct evidence that the poly(A) tail of influenza A virus mRNA is synthesized by reiterative copying of a U track in the virion RNA template." *Journal of virology*, *73*(4), 3473-6.

Portela, A. and Digard, P. (2002). "The influenza virus nucleoprotein: a multifunctional RNA-binding protein pivotal to virus replication." *The Journal of general virology*, *83*(Pt 4), 723-34.

Rao, P., Yuan, W et al.(2003). "Crucial role of CA cleavage sites in the cap-snatching mechanism for initiating viral mRNA synthesis."*The EMBO journal*, *22*(5), 1188-98.

Rehwinkel, J., Tan, C. P et al.(2010)." RIG-I detects viral genomic RNA during negative-strand RNA virus infection." *Cell*, *140*(3), 397-408.

Rothenfusser, S., Goutagny, N et al. (2005)." The RNA Helicase Lgp2 inhibits TLR-independent sensing of viral replication by Retinoic-acid-inducible gene-I." *The Journal of Immunology, 175,* 5260-5268.

Saito, T., Hirai, R et al.(2007)." Regulation of innate antiviral defenses through a shared repressor domain in RIG-I and LGP2." *Proceedings of the National Academy of Sciences of the United States of America*, *104*(2), 582-7.

Satoh, T., Kato, H et al. (2010)." LGP2 is a positive regulator of RIG-I- and MDA5-mediated antiviral responses." *Proceedings of the National Academy of Sciences of the United States of America*, *107*(4), 1512-7.

Scheiffele, P., Rietveld, A et al. (1999). "Influenza viruses select ordered lipid domains during budding from the plasma membrane." *The Journal of biological chemistry*, *274*(4), 2038-44.

Schlee, M., Roth, A et al. (2009). "Recognition of 5' triphosphate by RIG-I helicase requires short blunt double-stranded RNA as contained in panhandle of negative-strand virus." *Immunity*, *31*(1), 25-34.

Schmidt, A., Schwerd, T et al. (2009)." 5'-triphosphate RNA requires base-paired structures to activate antiviral signaling via RIG-I." *Proceedings of the National Academy of Sciences of the United States of America*, *106*(29), 12067-72.

Sedyaningsih, E. R., Isfandari, S et al.(2007). "Epidemiology of cases of H5N1 virus infection in Indonesia, July 2005-June 2006." *The Journal of infectious diseases*, *196*(4), 522-7.

Seo, S. H., Hoffmann, E et al.(2002). "Lethal H5N1 influenza viruses escape host anti-viral cytokine responses." *Nature medicine*, *8*(9), 950-4.

Shapiro, G. I and Krug, R M. (1988). "Influenza virus RNA replication in vitro: synthesis of viral template RNAs and virion RNAs in the absence of an added primer." *Journal of virology*, *62*(7), 2285-90.

Silverman R. H. (2007). "A scientific Journey Through the 2-5A/RNase L System." *Cytokine Growth Factor Rev*, *18*(5-6), 381-388.

Skehel, J. J. and Wiley, D. C. (2000). "Receptor binding and membrane fusion in virus entry: the influenza hemagglutinin." *Annual review of biochemistry*, *69*, 531-69.

Subbarao, K., Klimov, A et al.(1998)."Characterization of an avian influenza A (H5N1) virus isolated from a child with a fatal respiratory illness." *Science*, *279*(5349), 393-396.

Suhara, W., Yoneyama, M et al. (2002). "Direct involvement of CREB-binding protein/p300 in sequence-specific DNA binding of virus-activated interferon regulatory factor-3 holocomplex." *The Journal of biological chemistry*, *277*(25), 22304-13.

Takahasi, K., Kumeta, H et al. (2009)." Solution structures of cytosolic RNA sensor MDA5 and LGP2 C-terminal domains: identification of the RNA recognition loop in RIG-I-like receptors." *The Journal of biological chemistry*, *284*(26), 17465-74.

Talon, J., Horvath, C. M et al. (2000). "Activation of Interferon Regulatory Factor 3 Is Inhibited by the Influenza A Virus NS1 Protein Activation of Interferon Regulatory Factor 3 Is Inhibited by the Influenza A Virus NS1 Protein." *The Journal of Virology, 74* (17), 7989-7996.

Tanaka, H., Park, C.-H et al.(2003)." Neurotropism of the 1997 Hong Kong H5N1 influenza virus in mice." *Veterinary Microbiology*, *95*(1-2), 1-13.

Thompson, M. R., Kaminski, J. J et al.(2011)." Pattern Recognition Receptors and the Innate Immune Response to Viral Infection." *Viruses*, *3*(6), 920-940.

Twu, K. Y., Kuo, R.-L et al.(2007). "The H5N1 influenza virus NS genes selected after 1998 enhance virus replication in mammalian cells." *Journal of virology*, *81*(15), 8112-21.

Twu, K. Y., Noah, D. L et al. (2006). "The CPSF30 Binding Site on the NS1A Protein of Influenza A Virus Is a Potential Antiviral Target."*Journal of Virology*, *80*(8), 3957-3965.

Uyeki, T. M. and Bresee, J. S. (2007). "Detecting Human-to-Human Transmission of Avian Influenza A." *Emerg. Infect. Dis*, *13*(12), 1969-1971.

Venkataraman, T., Valdes, M et al.(2007)." Loss of DExD/H box RNA helicase LGP2 manifests disparate antiviral responses." *Journal of immunology*, *178*(10), 6444-55.

Vitour, D. and Meurs, E. F. (2007). "Regulation of interferon production by RIG-I and LGP2: a lesson in self-control." *Science's STKE : signal transduction knowledge environment*, *2007*(384),pe20.

Vong, S., Coghlan, B et al. (2006). "Low frequency of poultry-to-human H5NI virus transmission, southern Cambodia, 2005." *Emerging infectious diseases*, *12*(10), 1542-7.

Vreede, F. T., Jung, T. E et al. (2004). "Model Suggesting that Replication of Influenza Virus Is Regulated by Stabilization of Replicative Intermediates". *Journal of Virology*, *78*(17), 9568-9572.

Du, W., Thanos, D et al. (1993). "Mechanisms of trancriptional synergism between distinct virus-inducuble enhancer elements." *Cell*, *74*(5), 887-898.

Wang, C., Takeuchi, K et al. (1993). "Ion channel activity of influenza A virus M2 protein: characterization of the amantadine block." *Journal of virology*, *67*(9), 5585-94.

Wang, W., Riedel, K et al.(1999). "RNA binding by the novel helical domain of the influenza virus NS1 protein requires its dimer structure and a small number of specific basic amino acids . RNA binding by the novel helical domain of the influenza virus NS1 protein requires its dimer structure." *RNA*, *5*, 195-205.

Wang, X., Zhao, J et al. (2010). "Viremia associated with fatal outcomes in ferrets infected with avian H5N1 influenza virus." *PloS one*, *5*(8), e12099.

Webster, R. G., Bean, W. J et al.(1992)." Evolution and ecology of influenza A viruses." *Microbiological reviews*, *56*(1), 152-79.

Whittaker, G. R. (2001)." Intracellular trafficking of influenza virus : clinical implications for molecular medicine." *Expert Reviews in Molecular Medicine*, (February), 1-13.

Wise, H. M., Foeglein, A et al. (2009). "A complicated message: Identification of a novel PB1-related protein translated from influenza A virus segment 2 mRNA." *Journal of virology*, *83*(16), 8021-31.

Yoneyama, M., Suhara, W et al. (1998). "Direct triggering of the type I interferon system by virus infection: activation of a transcription factor complex containing IRF-3 and CBP/p300." *EMBO*, *17*(4), 1087-95.

Yoneyama, M., Kikuchi, M et al. (2004). "The RNA helicase RIG-I has an essential function in double-stranded RNA-induced innate antiviral responses." *Nature immunology*, *5*(7), 730-7.

Yoneyama, M., Kikuchi, M et al. (2005). "Shared and unique functions of the DExD/H-box helicases RIG-I, MDA5, and LGP2 in antiviral innate immunity." *Journal of immunology*, *175*(5), 2851-8.

Yoneyama, M. and Fujita T. " RIG-I family RNA helicases: Cytoplasmic sensor for antiviral innate immunity". *Cytokine Growth Factor, 18*, 545-551.

Yuan, P., Bartlam, M et al. (2009). "Crystal structure of an avian influenza polymerase PA(N) reveals an endonuclease active site." *Nature*, *458*(7240), 909-13.

Yuanji, G and Desselberger, U. (1984). "Genome analysis of influenza C viruses isolated in 1981/82 from pigs in China." *The Journal of general virology*, *65* (11), 1857-72.

Zeng, W., Sun, L et al. (2010). "Reconstitution of the RIG-I pathway reveals a signaling role of unanchored polyubiquitin chains in innate immunity." *Cell*, *141*(2), 315-30.